Review Article

Recent Progress, Advancements, and Efficiency Improvement Techniques of Natural Plant Pigment-Based Photosensitizers for Dye-Sensitized Solar Cells

Eneyew Tilahun Bekele [iD] **and Yilkal Dessie Sintayehu** [iD]

Department of Applied Chemistry, School of Applied Natural Science, Adama Science and Technology University, P.O. Box 1888, Adama, Ethiopia

Correspondence should be addressed to Eneyew Tilahun Bekele; eneyewtilahun77@gmail.com
and Yilkal Dessie Sintayehu; yilikaldessie@gmail.com

Production of green energy by using environment friendly and cost-effective components is attracting the attention of the research world and is found to be a promising approach to replace nonrenewable energy sources. Among the green energy sources, dye-sensitized solar cells (DSSCs) are found to be the most alternative way to reduce the energy demand crises in current situation. The efficiency of DSSCs is dependent on numerous factors such as the solvent used for dye extraction, anode and cathode electrodes, and the thickness of the film, electrolyte, dye, and nature of FTO/ITO glasses. The efficiency of synthetic dye-based DSSCs is enhanced as compared to their counterparts. However, it has been found that many of the synthetic sensitizers used in DSSCs are toxic, and some of them are found to cause carcinogenicity in nature by forming a complex agent. Instead, using various parts of green plants such as leaves, roots, steam, peel waste, flowers, various spices, and mixtures of them would be a highly environmentally friendly and good efficient. The present review focuses on and summarizes the efficiency affecting factors, the various categories of natural sensitizers, and solvent effects. Furthermore, the review work assesses the experimentally and computationally obtained values and their progress in development.

1. Introduction

Energy is an important and basic pillar of life activities across the globe. Basically, it exists in different forms, from burning woods to obtain fire in prehistoric times to producing electricity in modern society. But it has been found that the original sources of energy that people used to harvest in their day-to-day activities have shown signs of deficiency due to the rapid growth in industrialization, overgrowth in population size, the advancement of infrastructure, and humans' basic need improvement [1]. Due to uprising concerns about the energy crisis, climate change, shortages in fossil fuels, and current environmental issues are motivating the researcher to focus on clean, sustainable, and renewable energy resources that will help to predict future sustainability. Previously, it has been reported that energy produced from nonrenewable products had contributed to almost one-third of global greenhouse gas emissions [2, 3].

Nonrenewable energy products from fossil fuels, petroleum liquids, coal, and natural gas have been considered as the dominant source of energy production for the world economy in the past century. However, in view of nonrenewable energy sources such as the fossil fuel crisis, the rising per barrel cost of crude oil, and the rejection of pollution-causing energy sources, sustainable forms of energy are becoming the center of attention worldwide [4–6].

1.1. Renewable Sources of Energy. The common conventional sources of energy based on oil, coal, and natural gas have

proven to be highly efficient and effective product for economic progress but they might result in damaging the natural ecosystem and human health too. The fast depletion of fossil fuels and climate change issues and renewable energy sourced from solar, wind, geothermal, hydroelectric, biomass, nuclear power, and tide are some of the examples that are available in common throughout the world [7]. Renewable energy sources can provide sustainable energy service based on the use of routinely available starting materials and indigenous resources, which is available within the natural environment with minimum cost [8–10]. Solar energy provides a clean, renewable, and cheaper energy source for the human race. These concepts were supported by the world's energy consumption history projections covering the years from 1990 to 2040. From this projection, more than 60% of energy is dominated by solar energy in the years between 2090 and 2100 [11]. So, Figure 1 describes some common categories of both renewable and nonrenewable energy sources.

Energy from sunlight is capable of producing heat and light, causes photochemical reactions, and generates electricity. When sunlight strikes the earth's surface, it provides 3.8 million EJ of energy a year (i.e., collecting the total solar energy in one hour would satisfy human energy demand for one year) [12]. Light energy conversion applications are divided into three categories: photovoltaics for direct conversion of sunlight into electricity, as well as concentrating solar power systems and solar thermal collectors, employing solar thermal energy. All of this energy was modeled in an attempt to produce an efficient power output [11]. Photovoltaic (PV) technology has sparked a lot of interest due to the benefits of lower manufacturing costs and environmental safety. Its panel efficiency strongly depends on the surface temperature of the cell, and its efficiency decreases with increasing temperature [13].

Up to now, commercially available PV technologies are based on inorganic materials, which require high costs and highly energy-consuming preparation methods. In addition, several of those materials are toxic and have low natural abundance. Organic PV can be used to avoid those problems. However, the efficiencies of organic-based PV cells are still, at the moment, a long way behind those obtained with purely inorganic-based PV technologies. Hence, the benefit and significance of solar energy is that sunlight can be directly harvested into solar energy with the use of small and tiny PV solar cells [14]. Among silicon-based polymer, quantum dots, dye-sensitized solar cells, and perovskites are some of them and attract the researchers worldwide [15, 16]. Figure 2 demonstrates the classification of solar cells based on the materials on which they are made.

2. Dye-Sensitized Solar Cells (DSSCs)

Before dye-sensitized solar cells (DSSCs), silicon-based solar cells were found to be the most popular and dominant source of energy [18]. These solid-state junction devices dominated the photovoltaic industry. O'Regan and Grätzel [19] developed DSSCs, a new type of third-generation solar cell in year 1991 and also known as green alternative energy

due to its potential applications and cost-effectiveness. Moreover, this class of energy involves the use of green alternative solvents during its fabrication and does not result in the formation of pollution to the natural environment such as greenhouse gases, and the source by itself is uniformly distributed as compared to other forms of energy. One of the most operational technologies in this generation is its long-term stability and environmentally friendly energy that belongs to thin-film solar cell group [19, 20]. DSSCs are thus considered as one of the most promising next-generation devices for future energy demand and environmental remediation solutions. Its basic components include porous semiconductor materials loaded with sensitizer on a glass substrate (FTO/ITO), redox couple electrolyte, and counterelectrode [21, 22].

One form of modification made by previous researchers and reporters in the working electrodes is to add metal and metal-based oxide materials to semiconductors such as metals like Cr, Zr, Ni, Fe, Cu, Ag, CuO, ZnO, and TiO$_2$ [23, 24]. In addition to this, there are a number of factors limiting the performance of DSSCs. As such, the absorption of a large fraction of incident solar light by the photoactive layer of a dye-sensitized photoanode, the use of wide light absorption bands, and cosensitization of the photoanode are important for achieving high-performance and efficient device. Ragoussi and Torres also reported on the molecular orbital levels, absorption coefficients, morphology of the layers, and molecular diffusion lengths as the other main factors that affect certified power conversion efficiency [25].

Figures 3(a) and 3(b) illustrate the fundamental operational principle of DSSCs and the resulting charge transfer process between the sensitizer and the photoelectrode system. As described in Figure 3(a), sensitizers may achieve charge injection with the corresponding photoelectrode by both direct and indirect sensitization, as shown in Figure 3(b), thereby rendering it more panchromatic in response [26], and this showed the charge collection properties of DSSCs, which, in turn, altered the photocurrent density, photovoltage, and solar energy conversion efficiency by optimizing cell size without affecting environmental safety [27]. However, it has not yet come to fruition; pure direct sensitization protocol should be adapted, since it could increase DSSC efficiency by eliminating the electron injection overpotential. It indicates the energy loss due to thermalization from the excited state of the dye (D*) in the other process (indirect technique) [28].

Previously, much scientific research work was reported on the fabrication and assembly of DSSCs using their various components such as working electrode, counterelectrode, sensitizers/dyes (natural, organic metal free dye, and metal complex dyes/inorganic dyes), and the corresponding cell performance [30–34]. This is due to its best performance under solar irradiation diffusion, having low-cost manufacturing, fabrication simplicity, and environmental friendliness incorporated materials. But the low energy conversion and short-term operational stability are still a challenge for commercial use as compared with silicon-based solar cells, which have been commercialized [35].
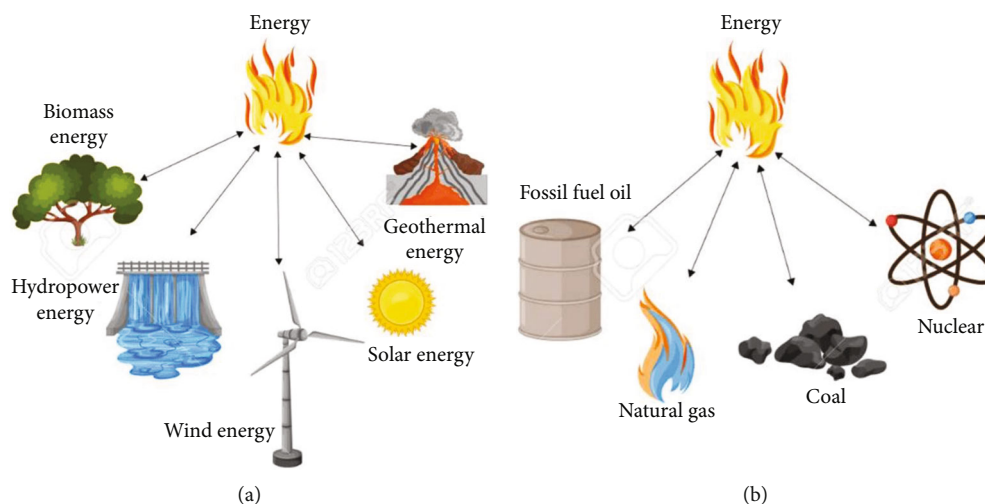
FIGURE 1: Education chart of (a) renewable and (b) nonrenewable sources of energy diagram (copyright: Vecton, image ID: 98899382, media type: stock photo).
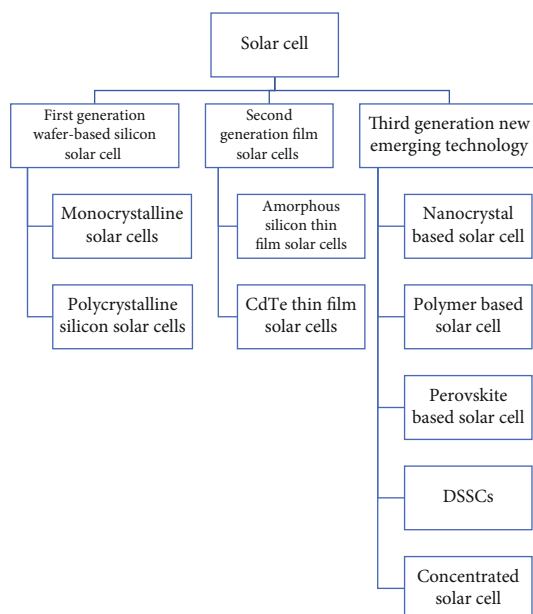

FIGURE 2: Category of solar cells and current trends of development [17].

However, to the knowledge of the researchers, there is no scientific report that summarizes and shows the effect of various components of the cell. Moreover, the novelty of this review work also focuses on showing and focusing on the different types of natural products as green, environmentally friendly, and cost-effective sensitizers for DSSCs. Furthermore, the work intends to summarize the effect of solvent on the extraction of dye and the effect and nature of the different parts of natural plants, such as roots, flowers, stems, and leaves, due to their having various bioactive photosensitive molecules [24, 36]. Hence, the aim of this review is to focus on performance affecting parameters, to show the recently achieved solar cell efficiency, to propose future scientific directions on the way to use DSSCs for homemade applications, and to extend their industrializations as well as its assessment on how to optimize the device for commercialization at large-scale production.

3. Basic Elements of DSSCs

In the old generation of photoelectrochemical solar cells (PSCs), photoelectrodes were fabricated from bulky semiconductor materials such as Si, GaAs, or CdS. But these kinds of photoelectrodes are highly affected by photocorrosion, which results in poor stability of the photoelectrochemical cell [37]. Instead, sensitized wide band gap semiconductors derived from metal oxides such as TiO_2, ZnO, niobium oxide, carbon materials, bilayer-assembled, and their composites have been used as a major photoelectrode in DSSCs, as shown in Figure 4 [38, 39]. So, the next section discussed the basic structure of DSSCs, which is composed of different layers as compared to conventional solar cells based on silicon, such as photoanode/photoelectrode/working electrode (WE), counterelectrode (CE), electrolyte, and sensitizer (both synthetic/complex and natural dyes) [35, 38, 40, 41].

3.1. Photoanode. The WE, or indicator, is the most important component that has the function of absorbing radiation. As a criterion, the electrode consists of a dye-sensitized layer of nanocrystalline semiconductor metal oxide having a wide band gap and being transparent enough to pass light to the sensitizer. Many semiconductor materials, either in the form of nano or bulk, were used as a photoelectrodes, such as TiO_2, $Al@TiO_2$, TiO_2-Fe, ZnO, SiO_2, Zn_2SnO_4, CeO_2, WO_3, $SrTiO_3$, and Nb_2O_5 were used as scaffold materials in DSSCs [26]. However, reports showed that TiO_2 and ZnO and their composite/doped-based photoelectrodes were found to be the most widely common photoanode materials due to their high band gap energy, inexpensiveness, nontoxicity nature, accessibility, and photoelectrochemical stability. Their methods of preparation are too simple and achievable
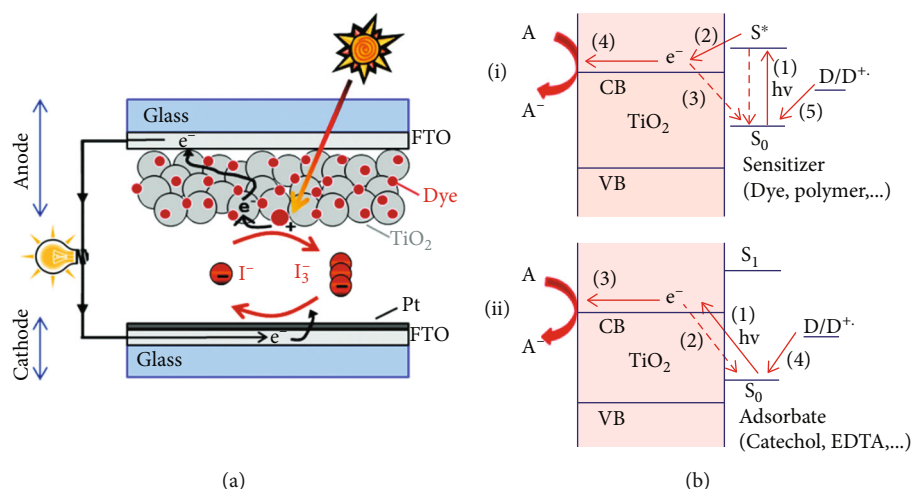
(a)

(b)

FIGURE 3: Schematic representation of the components and of the basic operating principle of DSSCs [29] (a) and the schematic illustration of two similar types of visible light sensitization of TiO_2. (i) Dye sensitization (indirect): (1) excitation of the dye by visible light absorption, (2) electron transfer from the excited state of the dye to TiO_2 CB, (3) recombination, (4) electron transfer to the acceptor, and (5) regeneration of the sensitizer by an electron donor. (ii) Ligand-to-metal charge transfer (LMCT sensitization) (direct): (1) visible light-induced LMCT transfer, (2) recombination, (3) electron transfer to the acceptor, and (4) regeneration of adsorbates by an electron donor. S, D, and A represent the sensitizer (or adsorbate), electron donor, and electron acceptor, respectively (S_0: ground state, S^* and S_1: excited state of the sensitizer/adsorbate) (b) [28].
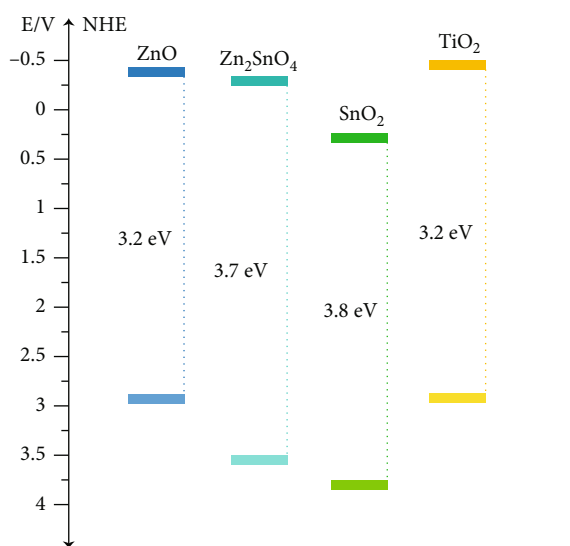

FIGURE 4: Band positions of the most common semiconductors [38].

with environmentally friendly materials in the presence of green solvents and show a promising high efficiency as compared to the counterparts. Recently, TiO_2 has become the most popular metal oxide semiconductor in DSSCs after ZnO and SnO_2 [38].

Rajendhiran et al. [42] have reported the green synthesized TiO_2 nanoparticles by the sol-gel method using *Plectranthus amboinicus* leaf extract, and the prepared nanoparticles have been coated over an ITO substrate by using the doctor blade approach. So, the assembled DSSCs have exhibited higher solar to electrical energy conversion efficiency, reaching 1.3% by using Rose Bengal organic dye

sensitizer due to the surface modification of the synthesized nanoparticles. In addition, to support TiO_2 in the photoanode, substrates such as fluorine-doped tin oxide (FTO) and indium-doped tin oxide (ITO) [9], due to scarcity, rigidity, and brittle properties of ITO, an alternative with low-cost FTO and graphene, have been chosen due to their unique structural defect with a rough surface that enables it to solve problems in short circuits and leakage current [39, 43].

Low and Lai [44] designed an efficient photoanode from reduced graphene oxide- (rGO-) decorated TiO_2 materials. It has been found that the UV-Vis diffuse reflection spectra shows an inconstant absorption with increasing duration of TiO_2 deposited on rGO in the ultraviolet (from 200 to 400 nm) and visible light (from 400 to 700 nm) regions. From the observed spectra, rGO/TiO_2 samples with a spinning duration of 30 seconds exhibited an optimum light-absorbing ability, as shown in Figure 5(a). As shown in Figure 5(b), the performance of the electrochemical parameters such as J_{SC}, V_{OC}, FF, and η was dependent on the spinning durations. The efficiency (η) of the assembled DSSCs increases from 10 to 30-second spinning duration (4.74-9.98%, respectively). This is due to surface area and photoelectrochemical stability modification, which in turn enables us to adsorb more dye molecules, followed by absorbing more light on the surface of the composite photoanode. So, it could be noticed that, after 30 seconds of optimized spinning duration, the best efficiencies of the device were 22.01 mA cm^{-2}, 0.79 V, 57%, 9.98% in J_{SC}, V_{OC}, FF%, and η %, respectively.

Furthermore, Gao et al. [45] also developed a nitrogen-doped TiO_2/graphene nanofiber (G-T-N) as an alternative green photoelectrode and evaluated the different
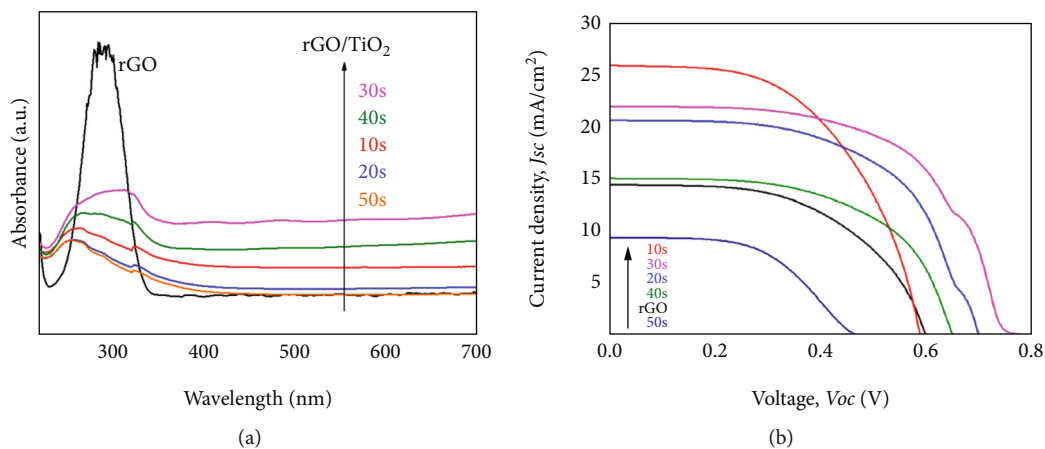
(a)

(b)

FIGURE 5: UV-Vis diffuses reflectance spectra (a) and J-V curves of the photoanode-based pure rGO and rGO/TiO$_2$ with spinning duration of 10 s, 20 s, 30, 40, and 50 s (b) [44].
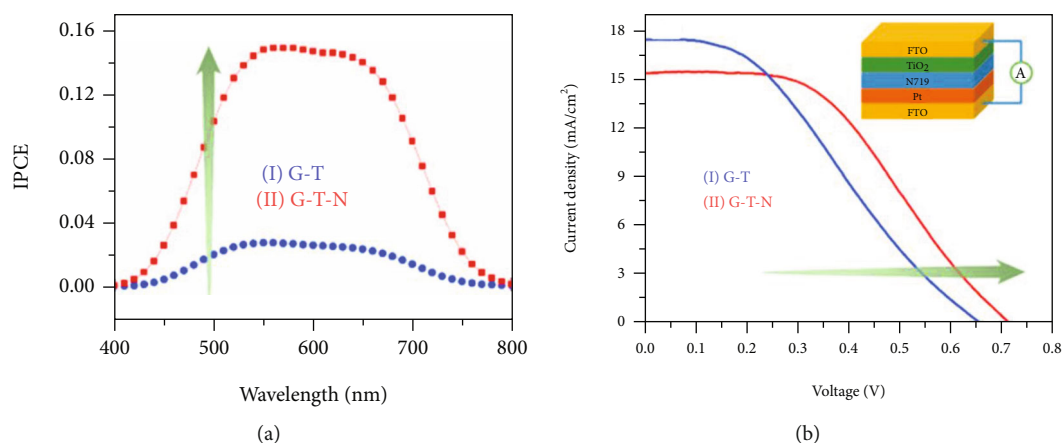

(a)

(b)

FIGURE 6: IPCE curves (a) and J-V curves of DSSCs with different photoanodes and the illustration in (b) [45].

photovoltaic parameters of the device's performance, as shown in Figure 6. While nitrogen doping can prevent the in situ recombination of electron-hole pairs, graphene doping first increases the surface area of TiO$_2$ fibers and also increases the dye adsorption active sites, with more electrons injected into the semiconductor conduction band from the excited state of the dye, thereby improving the photoelectric conversion efficiency. The open circuit voltage (V_{OC}), short circuit current density (J_{SC}), fill factor (FF), and η value for the TiO$_2$/graphene and N@TiO$_2$/graphene nanofiber photoelectrode-based DSSCs were found to be 0.66, 17.48, 0.35, and 3.97 and 0.71, 15.38, 0.46, and 5.01, respectively [46].

3.2. Counterelectrode. The counterelectrode (CE, cathode) is where the redox mediator reduction occurs. It collects electrons from the external circuit and injects them into the electrolyte to catalyze the reduction of I$_3^-$ to I$^-$ in the redox couple for dye regeneration [47]. The pillar and the primary major function of CE in the DSSC system plays as catalyst to promote the completion of the process, since

the oxidized redox couple is reduced by accepting electrons at the surface of the CE, and the oxidized dye is again reduced by collecting electrons *via* the ionic transport materials. The second ultimate role of CE in DSSCs is to act as a positive electrode; it collects electrons from the external circuit and transmits them into the cell. Additionally, CE is used as a mirror, since it reflects the unabsorbed light from the cell back to the cell to enhance the utilization of sunlight [40].

The most commonly used CE material is Pt on a conductive ITO or FTO substrate, owing to its excellent electrocatalytic activity for I$_3^-$ reduction, high electrical conductivity for efficient electron transport, and high electrochemical stability in the electrolyte system. Hence, most of the research work uses expensive platinum as a CE, but this limits the employability of large-scale production. Therefore, to address these limitations, several materials derived from inorganic compounds, carbonaceous materials, and conductive organic polymers, have been investigated as potential alternatives to replace or modify the Pt-based cathodes in DSSCs. To improve this, less-expensive copper was

used as the CE in large-scale industrial applications [39]. Huang et al. [48] have worked on biochar from lotus leaf by one-step pyrolysis as a flexible CE to replace platinum. From their studies at the same photoanode, a maximum value of 0.15% power conversion efficiency (PCE) was produced in the presence of lotus leaf extract as a photosensitizer, while 0.36% of PCE was produced. In the same manner, 0.13% of PCE was produced when graphite was used as CE while lotus leaf extract photosensitizer-modified TiO_2-FTO photoanode [48]. It can be concluded that graphite presents feasible potential as an alternative to platinum due to its affordable cost and performance output due to having more than 0.0385% efficiency than FTO glass and platinum by using *Strobilanthes cusia* photosensitizer [49].

Kumar et al. [50] designed and fabricated a new cost-effective, enhanced performance CE using a carbon material produced with the organic ligand 2- methyl-8-hydroxyquinolinol (Mq). The carbon-derived Mq CE-based DSSCs show a short circuit current density of $11.00 \, mA \, cm^{-2}$, a fill factor of 0.51, and an open circuit voltage of V_{OC} 0.75 V with a conversion efficiency of 4.25%. As a reference, Pt CE was used and provides a short circuit current density (J_{sc}) of $12.40 \, mA \, cm^{-2}$, a fill factor of 0.68, and an open circuit voltage of 0.69 V, having a conversion efficiency of $\approx 5.86\%$. As supported in Figure 7(a), the low cell performance of carbon-derived Mq CE could be attributed to the high electrostatic interactions between the carbon atom and I^- or I_3^- with a higher concentration of mediator anions in proximity to the carbon surface, which results in an increase of the regeneration and recombination rates [50]. Due to their low surface area, low stability, and low catalytic behavior, single material-based CE has lower device performance than composites and doped CE-based DSSCs. To improve this, Younas et al. [51] prepared the high meso-pore carbon-titanium oxide composite CE (HMC-TiO_2) for the first time and investigated the various cell photovoltaic parameters. The report shows that J_{sc} of $16.1 \, mA \, cm^{-2}$, FF of 68%, and V_{OC} of 0.808 V have a conversion η of $\approx 8.77\%$. As the different parameters of the DSSC value obtained show, the HMCs-TiO_2 composites display high electrocatalytic activity and could be taken as a promising CE. In addition, Song et al. [52] discuss the role of iron pyrite (FeS_2), in the presence and absence of NaOH basic solution, as one of the most promising counterelectrode materials for dye-sensitized solar cells. FeS_2 CE-based DSSCs without NaOH addition provides a PCE of 4.76%, a J_{SC} of $10.20 \, mA \, cm^{-2}$ with a V_{OC} of 0.70 V and a FF of 0.66. In the presence of NaOH, the FeS_2 CE-based DSSCs had a J_{SC} of $12.08 \, mA \, cm^{-2}$, a V_{OC} of 0.74 V, a FF of 0.64, and a PCE value of 5.78%. As a control, Pt CE were also investigated and shows J_{SC} of $11.58 \, mA \, cm^{-2}$, V_{OC} of 0.74 V, FF of 0.69, and resulting PCE of 5.93%. The improvement in the photovoltaic parameters of DSSCs, shown in Figure 7(b), indicates that more electrons are generated in the device due to the presence of NaOH, and this is found to be consistent with J_{SC} [53].

3.3. Electrolyte.

A good electrolyte should have high electrical and ionic conductivity, good interfacial contact with the nanocrystalline semiconductor and counterelectrode, not degrade the dye molecules, be transparent to visible light, noncorrosive property to the counterelectrode, high thermal and electrochemical stability, a high diffusion coefficient, low vapor pressure, appropriate viscosity, and ease of sealing, without suppressing charge carrier transport [54, 55]. Liquid electrolytes, solid-state electrolytes, quasisolid electrolytes [30], and water-based electrolytes [56] are common redox mediators (electrolytes) found in DSSCs. Liquid electrolytes are also organic (redox couple, a solvent, and additives) and are characterized by ionic liquid. Quasisolid electrolytes are good candidates for DSSCs due to their optimum efficiency and durability, high ionic conductivity, long-term stability, ionic conductivity, and excellent interfacial contact property like the liquid electrolytes. The most important components are redox couples such as I^-/I_3^-, Br^-/Br^{3-}, $SCN^-/(SCN)_2$, $Fe(CN)_6^{3/4}$, $SeCN^-/(SeCN)_2$, and substituted bipyridyl cobalt (III/II) [57], which are directly linked to the V_{OC} of DSSCs.

Due to the better solubility, fast dye regeneration process, low light absorption in the visible region, appropriate redox potential, and very slow recombination rate between the nanocrystalline semiconductor injected electrons and I_3^-, I^-/I_3^- is the most popular redox couple electrolyte [40]. Since a good solvent is responsible for the diffusion and dissolution of I^-/I_3^- ions, among these solvents, acrylonitrile, ethylenecarbonate, propylene carbonate, 3-methoxypropionitrile, and N-methylpyrrolidone are common. A solvent with a high donor number can increase the V_{OC} and decrease the J_{SC} by lowering the concentration of I_3^-. As a result, the lower I_3^- concentration helps to slow the recombination rate, and as a result, it increases the V_{OC}. The second type of liquid electrolyte is the ionic liquid electrolyte, such as pyridinium, imidazolium, and anions from the halide or pseudohalide family. These electrolytes show high ionic conductivity, nonvolatility, good chemical and thermal stability at room temperature, and a negligible vapor pressure, which are favorable for efficient DSSCs [30, 58]. Since, DSSCs are affected by evaporation and leakage found in liquid electrolyte. To overcome these drawbacks, novel solid or quasisolid state electrolytes, such as hole transportation materials, p-type semiconductors, and polymer-based gel electrolytes, have been developed as potential alternatives to volatile liquid electrolytes [59].

A quasisolid electrolyte is a means to solve the poor contact between the photoanode and the hole that transfers material found in solid-state electrolytes. This electrolyte is composed of a composite of a polymer and liquid electrolyte that can penetrate into the photoanode to make a good contact. Interestingly, this has better stability, high electrical conductivity, and especially, good interfacial contact when compared to the other types of electrolyte. However, the quasisolid electrolyte has one particular disadvantage: it is strongly dependent on the working temperature of the solar cell, where high temperatures cause a phase transformation from gel state to solution state. Selvanathan et al. [60] have used starch and cellulose derivative polymers as quasisolid
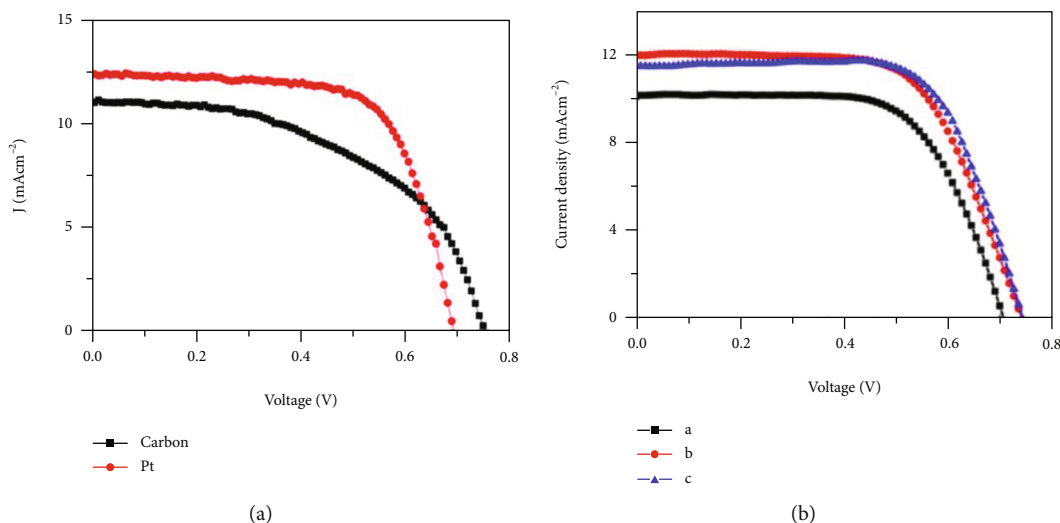
(a)

(b)

FIGURE 7: J-V spectra of HMC-TiO$_2$ (a) and FeS$_2$; (A: without NaOH, B: with NaOH, and C: Pt CE-based DSSCs) (b) [50, 52].

electrolytes and contributing to an optimized efficiency of 5.20% [60].

Saaid et al. [61] prepared a quasisolid-state polymer electrolyte by incorporating poly (vinylidene fluoride-co-hexafluoropropylene) (PVdF-HFP) into a propylene carbonate (PC)/1, 2-dimethoxyethane (DME)/1-methyl-3-propylimidazolium iodide (MPII) and dealing with the dependency of photovoltaic parameters on the fabricated electrolyte shown in Figure 8(a). It has been observed that the cell photovoltaic parameters are found to be dependent on the amount of the added PVDF-HFP polymer. Before the addition of any PVdF-HFP polymer, the corresponding Jsc, V_{OC}, FF, and η were found to be 11.24 mA cm^{-2}, 619 mV, 70%, and 4.88%, respectively. While followed by the addition of 0.1, 0.2, 0.3, and 0.4 g of PVdF-HFP polymer, the cell performance was found to be (9.53, 9.53, 7.54, and 6.57) mA cm^{-2} Jsc, (638, 641, 679, and 684) mV of V_{OC}, (67, 66, 64, and 61) % of FF, and (4.09, 3.70, 3.27, and 2.73) % of η, respectively. It was demonstrated that as the amount of polymer in the cell increases, the performance of the cell decreases gradually. Moreover, Lim et al. [62] have also designed a new quasisolid-state electrolyte using coal fly ash-derived zeolite-X and -A as shown in Figure 8(b) and achieves a V_{OC} of 0.74 V, J_{SC} of 13.7 mA/cm^2, and FF of 60% with η of 6.0% and 0.73 V, 11.4 mA/cm^2, 60% FF, respectively. But it has been found that zeolite-X&AF quasisolid-state electrolyte-based DSSCs show V_{OC} of 0.72 V, J_{SC} of 11.1 mA/cm^2, and FF of 61% and η of 4.8%. The enhancement in cell photovoltaic parameters in the case of zeolite-XF12 quasisolid-state electrolyte could be attributed to the high crystallinity nature, high light harvesting efficiency, the reduction of resistance at the photoanode/ electrolyte interface, and the decrease in charge recombination rate. As a control, nanogel polymer was used as an electrolyte and possessed 0.66 V, 10.3 mA/cm^2, 56% of FF, and 3.8% η.

3.4. Photosensitizer. Other core components of DSSCs are photosensitizers that play a great role in the absorption of solar photons. That is, dyes play a prominent role in harvesting the incoming light (absorbing) and injecting the photoexcited electrons into the conduction band of the semiconducting material to convert solar energy to electrical energy (i.e., which is responsible for absorbing the incident solar energy and converting it into electrical energy) [63, 64]. This enables us to produce renewable power systems and manage power sustainability and to achieve a reliable and stable network output power distribution [58]. It is chemically bonded to the porous surface of the semiconductor material and determines the efficiency and general performance of the device [47]. The possibilities of some organic dyes, polymer dyes, and natural dyes have been reported with great relative cost-effective potential for industrialization [11]. To be effective, photosensitizer should have a broad and intense absorption spectrum that covers the entire visible region, high adsorption affinity to the surface of the semiconducting layer, excellent stability in its oxidized form, low-cost, and low threat to the environment. Furthermore, its LUMO level, i.e., excited state level, must be higher in energy than the conduction band edge of the semiconductor, for efficient electron injection into the conduction band of the semiconductor. Also, its HOMO level, i.e., oxidized state level, must be lower in energy than the redox potential of the electrolyte to promote dye regeneration .

The most commonly used photosensitizers are categorized into three groups. These are metal complex sensitizers, metal-free organic sensitizers [65], and natural sensitizers. Metal complex sensitizers provide relatively high efficiency and stability due to having both anchoring and ancillary ligands. The modifications of these two ligands to improve the efficiency of the solar cell performance have been reported. These ligands facilitate charge transfer in metal-to-ligand bonds. The metal complex-based photosensitizers are ruthenium and its cosensitized configurations [56] based complexes owing to their wide absorption range, i.e., from the visible to the near-infrared region, which renders them with superior photon harvesting properties. However, these complexes require multistep synthesis reactions (i.e., they
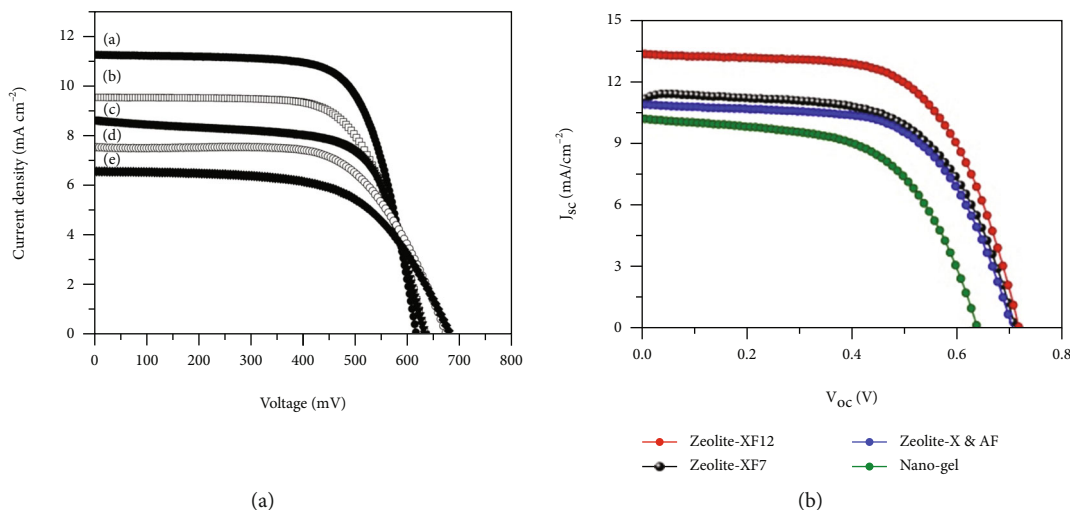
(a)

(b)

Figure 8: J-V curve of PVdF-HFP/PC/DME/MPII (a) with A 0.0; B 0.1; C 0.2; D 0.3; and E 0.4 g of PVdF-HFP and photocurrent Density-photovoltaic curves of DSSCs based on nanogel and quasisolid-state electrolytes under 1 sun illumination (AM 1.5G, $100 \, mW \, cm^{-2}$) (b) [48, 49].

require long synthesis and purification steps), and they contain a heavy metal, which is expensive (i.e., it needs high production costs), scarce, and toxic. However, these problems can be overcome by applying metal-free organic dyes in DSSCs instead of metal complex sensitizers. Trihutomo et al. [66] explained that using natural dye as a photosensitizer has the problem of producing lower efficiency than silicon solar cells due to the barrier of electron transfer in the TiO_2 semiconductor layer.

A donor acceptor-substituted-conjugated bridge (D-π-A) is used in the design of a metal-free organic sensitizer [30, 47]. The properties of a sensitizer vary with the electron-donating ability of the donor part and the electron-accepting ability of the acceptor part, as well as with the electronic characteristics of π bridge. At present, most of the π-bridge conjugated parts in organic sensitizers are based on oligoene, coumarin, oligothiophene, fluorene, and phenoxazine. The donor part has been synthesized with a dialkyl amine or diphenylamine moiety while using a carboxylic acid, cyanoacrylic acid, or rhodanine-3-acetic acid moiety for the acceptor part. As shown in Figure 9 [30], the sensitizer anchors onto the porous network of nanocrystalline TiO_2 particles via the acceptor part of dye the molecule. However, metal-free organic sensitizers (organic dyes) have the following disadvantages: strong π-stacked aggregates between D-π-A dye molecules on semiconductor surfaces, which reduces the electron-injection yield from the dyes to the conduction band of nanocrystalline semiconductor, low absorption bands compared to metal-based sensitizers, which leads to a reduction in light absorption capability, low stability due to the sensitizer's tendency to decay with time, and a long anode lifetime [30, 67].

In brief, the 3.2 eV energy band gap of the TiO_2 semiconductor is responsible for absorbing ultraviolet light (i.e., the absorption of visible light is weak). As a result, natural dyes increase the overall DSSCs for sunlight absorption rate [68].

The light-absorbed efficiency by TiO_2 is also enhanced by cosensitization, which enables better light harvesting across the solar spectrum [69]. Ananthakumar et al. [70] have also reviewed more on the energy transfer process from donor to acceptor through the Forster resonance energy transfer process (FRET) for improved absorption. So, cosensitization is effectively achieved through the FRET mechanism, in which the dipole-dipole attraction of two chromophoric components occurs via an electric field. In this process, absorption of light causes the molecular excitation of the donor, and this is transferred to a nearby acceptor molecule having lower excitation energy through the exchange of virtual photons. Here, the donor molecule nonradiatively transfers excitation energy to an acceptor molecule through an exchange of photons, as shown in Figure 10 [70].

To solve problems found in both metal-based complex and metal-free organic dyes, researchers have focused on natural plant pigment-based photosensitizer [71]. As a result, metal-free dyes, such as natural dyes (natural pigments) from different plant sources such as fruits, roots, flowers, leaves, wood, algae, and bacterial pigments [72, 73], coupled with their organic derivatives, have attracted considerable research interest, owing to their low-cost, simple synthesis procedure, abundance in nature, nontoxicity, and high molar absorption coefficient [35, 74]. An efficient photosensitizer for DSSCs should possess several essential requirements [64]:

  (i) A high molar extinction coefficient and a high panchromatic light absorption ability that extends from visible to near-infrared

  (ii) Anthocyanin pigment from *Eleiodoxa conferta* and *Garcinia atroviridis* fruit, for example, contains hydroxyl and carboxylic groups in the molecule that can effectively attach to the surface of a TiO_2 film [75]
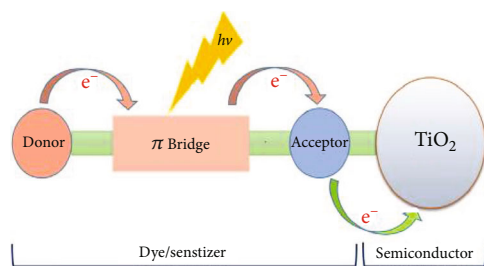
FIGURE 9: Designed structure of a metal-free organic dye [30].

(iii) Good HOMO/LUMO energy alignment with respect to the redox couple and the conduction band level in the semiconductor, which allows efficient charge injection into the semiconductor, and simultaneously efficient regeneration of the oxidized dye

(iv) The electron transfer rate from the dye sensitizer to the semiconductor must be faster than the decay rate of the photosensitizer

(v) Stability under solar light illumination and continuous light soaking [76–78]

It is important to note that the stable natural plant pigments extracted by effective solvents can absorb a broad range of visible light [79, 80], because the two most significant drawbacks of DSSCs are their narrow spectral response and short-term stability. Therefore, in this review work, different natural plant pigments are extracted from different plant parts such as leaves, roots, steam, parks, peel waste, flowers, various spices, and a mixture of them with various solvents, and their stability and various experimental factors are effectively discussed.

3.4.1. Natural Plant Pigment Photosensitizers in DSSCs. The highest efficiency ever recorded for a DSSCs material was about 12% using Ru (II) dyes when its material and structural properties were optimized. However, this efficiency is less when compared to the efficiencies of the first and second generations of solar cells (thin-film solar cells and first generation (Si-based) solar cells), whose efficiencies were about 20-30% [11]. A ruthenium-based dye and platinum are the most common materials used as photosensitizer and counterelectrode, respectively, in the production of the DSSCs, the third generation of photovoltaic technologies. However, their expensive cost, the complexity and toxicity of ruthenium dye, and the scarcity of platinum sources preclude their use in the DSSCs [49]. Thus, an alternative way to produce cost-effective dyes on a large scale is by extracting natural dyes from plant sources. The colors are due to the presence of various pigments that have been proven to be efficient photosensitizers. Meanwhile, colors and their transmittance by themselves could affect energy generation performance. Based on this, DSSCs currently being produced have better power generation efficiency as the visible light transmittance lowers, and the power generation efficiency

is good in the order of red > green > blue [81]. It is reported that extracts of plant pigments also have a simultaneous effect as photosensitizers and reducing agents for nanostructure synthesis, which is useful in photoanode activity in solar devices (e.g., TiO_2) [82].

In order to improve the energy conversion efficiency of natural photosensitizers, blending of different dyes, copigmentation of dyes, acidifying of dyes, and other approaches have been conducted by researchers, resulting in appreciable performance [83]. Based on the types of natural molecules found in plant products, such photosensitizers are classified as carotenoids, betalains, flavonoids, or chlorophyll structural classes [30, 65, 83, 84]. For stable adsorption onto the semiconductor substrate, sensitizers are typically designed with functional groups such as -COOH, $-PO_3H_2$, and $-B(OH)_2$ [20]. These biomolecules have functional groups, such as carboxyl and hydroxyl that can easily react with the surface of nanostructured TiO_2 that enables them to absorb sunlight. In particular, hydroxyl or carboxyl functional groups are strongly bound on the surface of TiO_2 [85].

The enchantment of efficiency from extraction of dyes from fresh purple cabbage (anthocyanin), spinach leaves (chlorophyll), turmeric stem (betaxanthin), and their mixture as a photosensitizer, with nanostructured ZnO-coated FTO substrates as a photoanode-based DSSCs. The photon to electrical power conversion efficiencies of purple cabbage, spinach, turmeric, and their mixed dyes are explored as 0.1015%, 0.1312%, 0.3045%, and 0.602%, respectively, under the same simulated light condition. The mixed dye reveals the stable performance of the cell with the highest conversion efficiency due to the absorption of an extensive range of the solar spectrum and well-suited electrochemical responses due to the fast electron transportation and lower recombination loss with longer electron lifetime found on mixed dyes [86].

(1) Flowers. In DSSCs, the red/purple pigment in various leaves and flowers has been used as a sensitizer. Notably, an abundantly available organic dye is easily extracted from flowers and leaves, mainly responsible for light absorption in DSSCs [39]. The natural color pigments originated from organic dyes impart an anthocyanin group present in the different parts (e.g., flowers, leaves) of the plant. *Hibiscus rosa-sinensis*, a red pigment-containing flower with a higher concentration of anthocyanins, is used as a natural DSSC. In fact, the *Malvaviscus penduliflorus* flower is closely related to the *Hibiscus* family. However, potential research based on *M. penduliflorus* flower extracted dye in DSSCs is still lacking. The broader absorption of *Hibiscus*-extracted dye within 400-500 nm can further be enhanced using either concentrated dye solution or operating the sensitization process at an elevated temperature [39].

Natural dyes from flowers can decrease the charge transfer resistance and are helpful in the better absorbance of light as well as enabling them to show absorption near to the red region. Therefore, efficient DSSCs using natural dyes are less toxic, disposed of easily, cost-effectively, and more environmentally friendly compared to organic dyes. Which
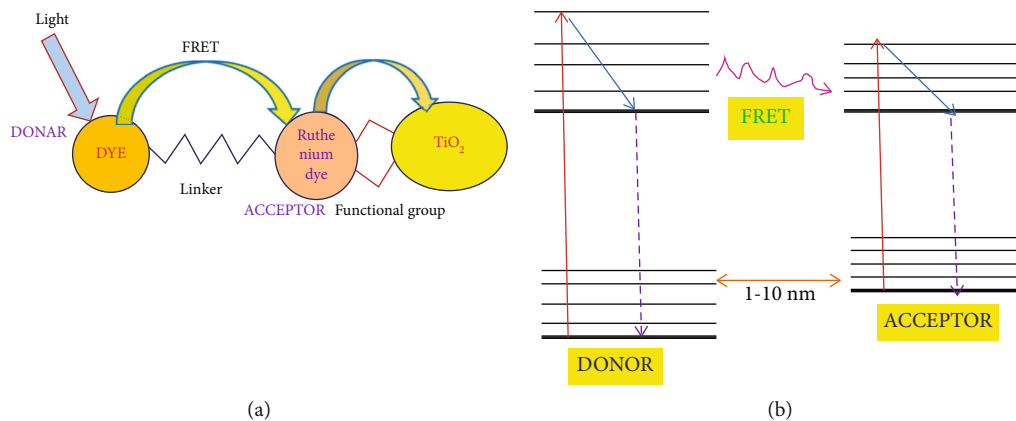
FIGURE 10: Schematic diagram of FRET process (a) and its mechanism (b) [70].

is considered beneficial for future biosolar cell technology [87]. The performance of the DSSCs can be compensated by introducing a scattering layer or interfacial modification in the photoanode and concomitantly improving the broader spectrum wavelength range of light absorption to make it suitable for outdoor applications [39]. the presence of a series of conjugated double bonds from flower extracts helped to increase efficiency improvement. Raguram and Rajni [88] demonstrated that a flavanol pigment from the *Allamanda blanchetti* flower is responsible for red, purple, and blue colors, whereas a carotenoid pigment from the *Allamanda cathartica* flower is responsible for bright red, orange, and yellow colors and a series of conjugated double bonds [88]. Table 1 summarizes flower-based photosensitizers for efficiency improvement in DSSCs. From this, the performance is highly dependent on the type of the plant flower type.

(2) Leaves. The advantages of mesoporous holes in TiO_2 are that they provide the surface of a large hole for the higher adsorption of dye molecules and facilitate the penetration of electrolyte within their pores. Absorbing light in an extended range of wavelengths by innovative natural dyes followed by increasing surface areas of the photoanode with a TiO_2 nanostructure-based layer on the glass substrate improves DSSC technology [74]. Khammee et al. [89] have reported a natural pigment photosensitizer extracted from *Dimocarpus longan* leaves. According to the report, the methanol extract pigment was composed of chlorophyll-a, chlorophyll-b, and carotene components [89]. The functional group found on the leaves of natural plant pigment can bind with TiO_2, which is then responsible for absorbing visible light [54]. Chlorophyll, which is found in the leaves of most green plants, absorbs light from red, blue, and violet wavelengths and obtains its color by reflecting green. Chlorophyll exhibits two main absorption peaks in the visible region at wavelengths of 420 and 660 nm [85]. Experimental results show that the absorption peaks of those dyes are mainly distributed in the visible light regions of 400-420 nm and 650-700 nm. So, chlorophyll was selected as the reference dye [94]. Therefore, chlorophyll and other

related extract-based photosensitizes are given in both Tables 1 and 2.

(3) Fruits. The plant-extracted natural dyes are observed to be more prospective owing to their abundance and eco-friendly characteristics. They are environmentally and economically superior to ruthenium-based dyes because they are nontoxic and cheap. However, the conversion efficiency of dye-sensitized solar cells based on natural dyes is low [95]. Substations of natural dyes as sensitizers were shown to be not only economically viable and nontoxic but also effective for enhancing efficiency up to 11.9% [96]. Sensitizers for DSSCs need to fulfill important requirements such as absorption in the visible and near-infrared regions of the solar spectrum and strong chelation to the semiconductor oxide surface. Moreover, the LUMO of the dye should lie at a higher energy level than the conduction band of the semiconductor, so that, upon excitation, the dye could introduce electrons into the conduction band of the TiO_2 [95]. Considering this, Najm et al. [97] used abundant and cheap Malaysian fruit, betel nut (*Areca catechu*) as a photosensitizer in DSSCs due to the presence of tannins, polyphenols, gallic acid, catechins, alkaloids, fat, gum, and other minerals. Provided that, gallotannic acid, a stable dye, is the main pigment (yellowish) of *A. catechu* and is responsible for the effective absorption of visible wavelengths and used in DSSCs [97, 98]. So, fruit extract as a photosensitizer and natural extracts from other sources are summarized in Table 3 and 4, respectively.

The narrow spectral response and the short-term stability found in DSSCs are the two major drawbacks. These limitations are improved by using natural plant pigment dyes as an effective sensitizer on the photoanode of the device. So, using these natural pigments improved the efficiency of DSSCs by forming broad spectral absorption responses. To improve this, DeSilva et al. have investigated good photosensitizers from Mondo-grass berry and blackberry. As a result, the device efficiency improvement, with better stability on Mondo-grass berry dye, was observed when compared with that of blackberry. This is the reason that a Mondo-grass

TABLE 1: Flowers as photosensitizers in DSSCs.

Image	Plant	Class of biomolecules	Solvent for extraction	Photoanode	J_{sc} (mA cm^{-2})	V_{oc} (V)	FF (%)	η (%)	Ref
	Salvia	—	Methanol	TiO$_2$-FTO	0.168	0.461	40.0	0.152	[87]
	Spathodea	—	Methanol	TiO$_2$-FTO	0.201	0.525	41.2	0.217	[87]
	Malvaviscus penduliflorus	—	Ethanol	TiO$_2$/MnO$_2$-FTO	6.02	0.38	40.38	0.92	[39]
	Allamanda blanchetti	Flavonoids (flavanol)	Ethanol	TiO$_2$-FTO	4.1366	0.4702	60	1.16	[88]
	Allamanda cathartica	Carotenoids (lutein)	Ethanol	TiO$_2$-FTO	2.1406	0.4896	28	0.30	[88]
	Canna-lily red	Anthocyanins	Methanol	TiO$_2$-FTO	0.44	0.57	45	0.14	[90]
	Canna-lily yellow	Anthocyanins	Methanol	TiO$_2$-FTO	0.43	0.56	40	0.12	[90]
	Beta vulgaris L. ssp. *f. rubra*	Beta carotene	Hot water	TiO$_2$ surface	0.44	0.55	51	0.41	
	Brassica oleracea L. var. *capitata f. rubra*	Anthocyanin	Hot water	TiO$_2$ surface	1.88	0.54	56	1.87	

TABLE 2: Leaves as photosensitizers in DSSCs.

Image	Plant	Class of extracted dye pigments	Solvent for extraction	Photoanode	J_{sc} (mA cm^{-2})	V_{oc} (V)	FF (%)	η (%)	Ref
	Lagerstroemia macrocarpa	(i) Carotenoids (ii) Chlorophyll-a (iii) Chlorophyll-b	Methanol	TiO$_2$-FTO	0.092	0.807	53.71	1.138 ± 0.018	[74]
	Spinach leaves	(i) Chlorophyll	Acetone	TiO$_2$-FTO	0.41	0.59	58.75982	0.171253	[26]
	Strobilanthes cusia	(i) Chlorophyll-a (ii) Chlorophyll-b	Methanol, ethanol, acetone, diethyl-ether, dimethyl-sulphoxide	TiO$_2$-FTO	0.0051833	0.306	46.2	0.0385	[49]
	Galinsoga parviflora	(i) Chlorophyll group	Distilled water and ethanol	TiO$_2$-FTO	0.4 (mA)	0.3	46.7	1.65	[91]
	Amaranthus red	(i) Chlorophyll (ii) Betalain	Distilled water, ethanol, acetone	TiO$_2$-FTO	1.0042	0.3547	38.64	0.14	[54]
	Lawsonia inermis	(i) Lawsone (ii) Chlorophyll	Distilled water, ethanol, acetone	TiO$_2$-FTO	0.4236	0.5478	38.51	0.09	[54]
	Cordyline fruticosa	(i) Chlorophyll	Ethanol	TiO$_2$ surface	1.3 mA	0.616	60.16	0.5	[85]
	Euodia meliaefolia (Hance) Benth	(i) Chlorophyll	Ethanol	TiO$_2$-FTO	2.64	0.58	70	1.08	[92]
	Matteuccia struthiopteris (L.) Todaro	(i) Chlorophyll	Ethanol	TiO$_2$-FTO	0.75	0.60	72	0.32	[92]
	Corylus heterophylla Fisch	(i) Chlorophyll	Ethanol	TiO$_2$-FTO	0.68	0.56	69	0.26	[92]

TABLE 2: Continued.
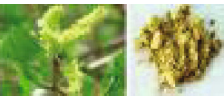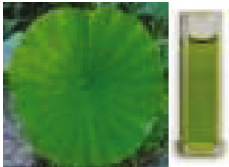
Image	Plant	Class of extracted dye pigments	Solvent for extraction	Photoanode	J_{sc} (mA cm^{-2})	V_{oc} (V)	FF (%)	η (%)	Ref
	Filipendula intermedia	(i) Chlorophyll	Ethanol	TiO$_2$-FTO	0.87	0.54	74	0.34	[92]
	Pteridium aquilinum var. latiusculum	(i) Chlorophyll	Ethanol	TiO$_2$-FTO	0.74	0.56	73	0.30	[92]
	Populus L	(i) Chlorophyll	Ethanol	TiO$_2$-FTO	1.25	0.57	37	0.27	[92]
	Euphorbia sp.	(i) Quercetin	Hot water	TiO$_2$ surface	0.46	0.40	51	0.30	
	Rubia tinctoria	(i) *Alizarin*	Hot water	TiO$_2$ surface	0.65	0.48	63	0.65	
	Morus alba	(i) *Cyanine*	Hot water	TiO$_2$ surface	0.44	0.45	57	0.38	
	Reseda lutea	(i) *Luteolin*	Hot water	TiO$_2$ surface	0.50	0.50	62	0.52	
	Medicago sativa	(i) *Chlorophyll*	Hot water	TiO$_2$ surface	0.33	0.55	56	0.33	
	Aloe barbadensis miller	(i) *Anthocyanins*	Ethanol	TiO$_2$-FTO	0.112	0.676	50.4	0.380	[93]
	Opuntia ficus-indica	(i) Chlorophyll	Ethanol	TiO$_2$-FTO	0.241	0.642	48.0	0.740	[93]

TABLE 2: Continued.

Image	Plant	Class of extracted dye pigments	Solvent for extraction	Photoanode	J_{sc} (mA cm^{-2})	V_{oc} (V)	FF (%)	η (%)	Ref
	Cladode and aloe vera	(i) Anthocyanins and chlorophyll	Ethanol	TiO$_2$-FTO	0.290	0.440	40.1	0.500	[93]
	Lotus leaf	(i) Alkaloid and flavonoid	Ethanol	TiO$_2$-FTO	14.33	0.44	23	1.42	[48]
	Brassica oleracea var	(i) Anthocyanin	Distilled water, methanol, and acetic acid	TiO$_2$-FTO	0.49	0.43	51	0.054	[55]
	Wrightia tinctoria R.Br. ("Pala indigo" or "dyer's oleander")	(i) Chlorophyll	Cold methanolic extract	TiO$_2$-FTO	0.53	0.51	69	0.19	[94]
		(i) Chlorophyll	Acidified cold methanolic extract	TiO$_2$-FTO	0.21	0.422	66	0.06	[94]
		(i) Chlorophyll	Soxhlet extract	TiO$_2$-FTO	0.49	0.495	69	0.17	[94]
		(i) Chlorophyll	Acidified Soxhlet extract	TiO$_2$-FTO	0.31	0.419	65	0.08	[94]

berry contains a mixture of two or more chemical compounds belonging to both the anthocyanin and carotenoid families, as proved by thin layer chromatography [105].

4. Photoinduced Electron Transfer Rate Efficiency in Natural Plant Pigment DSSCs

Anthocyanin coupled with TiO$_2$ is cheap, readily available, and innocuous to the environment, with high economic advantages over other types of photovoltaic devices, but it has yet to become a commercially viable product due to its low conversion efficiency and life span [11]. In addition, TiO$_2$ photoelectrode properties favor natural pigments as sensitized DSSCs because the conduction band of TiO$_2$ photoelectrode coincides well with the excited level LUMO of natural pigments (especially with anthocyanins) [106].

The interaction between TiO$_2$ and dye molecule could lead to the transfer of excited electrons from the dye molecules, to the conduction band of TiO$_2$ [85] as shown in Figure 11.

For good photovoltaic efficiency of a DSSC, an electron from the electronically excited state of the dye must be injected effortlessly into the conduction band of the semiconductor. The electron transfer kinetics of natural dye molecules can be appraised in terms of the photoinduced electron transfer (PET) theory. The theory implies that the logarithm of the electron transfer rate is a quadratic function with respect to the driving force, $-\Delta G \circ$. The simplified form of the rate constant of ET, k_{ET}, is given as follows:

$$k_{ET} = A \exp \left[\frac{(-\Delta G^o + \lambda)^2}{4\lambda RT} \right], \tag{1}$$

TABLE 3: Fruits as photosensitizers in DSSCs.
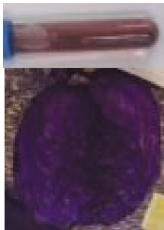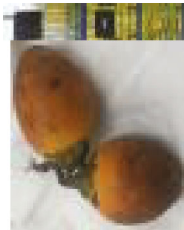
Image	Plant	Class of extracted dye pigments	Solvent for extraction	Photoanode	J_{sc} (mA cm^{-2})	V_{oc} (V)	FF (%)	η (%)	Ref
	Melastoma malabathricum	(i) Anthocyanin	Methanol and trifluoroacetic acid	TiO$_2$ film	4.49	0.42	57	1.05	[84]
	Eleiodoxa conferta	(i) Anthocyanin	Ethanol	TiO$_2$-FTO	4.63	0.37	56	1.00	[75]
	Garcinia atroviridis	(i) Anthocyanin	Ethanol	TiO$_2$-FTO	2.55	0.32	63	0.51	[75]
	Onion peels	(i) Anthocyanin	Distilled water	TiO$_2$-FTO	0.24	0.48	46.63	0.065	[26]
	Red cabbage	(i) Anthocyanin	Distilled water	TiO$_2$-FTO	0.21	0.51	46.61	0.060	[26]
	Areca catechu	Gallotannic acid	Methanol	TiO$_2$ surface	0.3	0.536	73.5	0.118	[97]

TABLE 3: Continued.
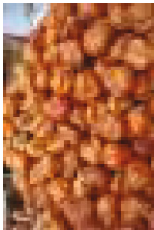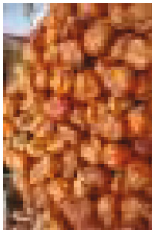
Image	Plant	Class of extracted dye pigments	Solvent for extraction	Photoanode	J_{sc} (mA cm^{-2})	V_{oc} (V)	FF (%)	η (%)	Ref
	Hylocereus polyrhizus	(i) Anthocyanin	Distilled water, ethanol, and acetic acid	TiO$_2$-FTO	0.23 mA	0.34	63	0.024	[55]
	Doum palm	(i) Chromophores	Ethanol	TiO$_2$-FTO	0.005	0.37	63	0.012	[99]
	Doum palm	(i) Chromophores	Distilled water	TiO$_2$-FTO	0.010	0.50	66	0.033	[99]
	Linia cauliflora	(i) Anthocyanin	Ethanol	TiO$_2$-ITO	0.38	0.41	29	0.13	[100]
	Phyllanthus reticulatus	(i) Anthocyanin	Methanol	TiO$_2$-FTO	1.382	0.67	—	0.69	[101]

TABLE 4: Other natural pigment sources as photosensitizers in DSSCs.
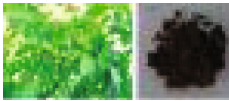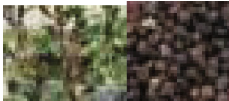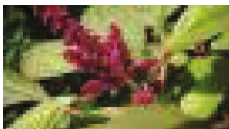
Image	Plant	Class	Solvent for extraction	Photoanode	J_{sc} (mA cm^{-2})	V_{oc} (V)	FF (%)	η (%)	Ref
	Juglon regia shell	(i) Juglon	Hot water	TiO$_2$ surface	0.43	0.47	56	0.38	
	Malabar spinach seeds	—	Distilled water	TiO$_2$-ITO	510 (μA)	0.710	48.7	9.23	[102]
	Rhamnus petiolaris seed	(i) Emodin	Hot water	TiO$_2$ surface	0.20	0.50	55	0.18	
	Iridaea obovata algae	(i) Phycoerythrin	Ethanol	TiO$_2$-FTO	0.136	0.40	43	0.022	[103]
	Delesseria lancifolia algae	(i) Phycoerythrin	Ethanol	TiO$_2$-FTO	0.243	0.40	46	0.045	[103]
	Plocamium hookeri algae	(i) Phycoerythrin	Ethanol	TiO$_2$-FTO	0.083	0.53	63	0.027	[103]
	Mangosteen pericarp (mangosteen peels)	(i) Anthocyanin	Ethanol	TiO$_2$-FTO	0.38 mA	0.46	48	0.042	[55]
	Ataco vegetable	(i) Anthocyanins	Ethanol	TiO$_2$-FTO	0.06	0.48	66	0.018	[104]
	Achiote vegetable	(i) Anthocyanins	Ethanol	TiO$_2$-FTO	0.06	0.45	50	0.013	[104]
	Berenjena vegetable	(i) Anthocyanins	Ethanol	TiO$_2$-FTO	0.04	0.40	56	0.008	[104]

TABLE 4: Continued.

Image	Plant	Class	Solvent for extraction	Photoanode	J_{sc} (mA cm^{-2})	V_{oc} (V)	FF (%)	η (%)	Ref
	Flor de Jamaica vegetable	(i) Anthocyanins	Ethanol	TiO$_2$-FTO	0.382	0.478	58	0.109	[104]
	Mora vegetable	(i) Anthocyanins	Ethanol	TiO$_2$-FTO	0.28	0.48	51	0.069	[104]
	Mortiño vegetable	(i) Anthocyanins	Ethanol	TiO$_2$-FTO	0.557	0.484	66.4	0.175	[104]
	Rabano vegetable	(i) Anthocyanins	Ethanol	TiO$_2$-FTO	0.07	0.39	55	0.015	[104]
	Tomate de arbol vegetable	(i) Anthocyanins	Ethanol	TiO$_2$-FTO	0.10	0.44	52	0.023	[104]

where $\Delta G\circ$ is the driving force, λ is the reorganization energy, R is the gas constant, and T is the temperature. In the region of driving force smaller than the reorganization energy (the normal region), the electron transfer rate increases as driving force increases. The electron transfer rate attains a maximum value at $\Delta G\circ = \lambda$. When the driving force for reaction is greater than λ, inverted region kinetics are observed, and the electron transfer rate decreases as the driving force increases .

The driving force for electron transfer between a photosensitizer and semiconductor nanoparticles can be dictated by the energy difference between the oxidation potential of the photosensitizer and the reduction potential of semiconductor nanoparticles. The Rehm-Weller equation can be utilized to determine the driving force energy changes for the PET process. This equation gives the driving force energy changes between a donor (D) and an acceptor (A) as [108]:

$$\Delta G^o = e[E_{Oxi.}(D) - E_{Red.}(A)] - \Delta E^*, \qquad (2)$$

where e is the unit electrical charge, $E_{Oxi.}(D)$ and $E_{Red.}(A)$ are the oxidation and reduction potentials of electron donor and acceptor, respectively. $\Delta E*$ is the electronic excitation energy that corresponds to the energy difference between the ground and first excited states of donor species .
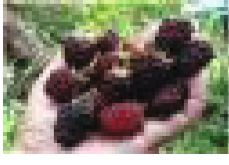
This is followed by regeneration of the dye by the redox mediator, transport of electrons in mesoporous TiO$_2$ and redox mediators in the electrolyte, and finally, reduction of the oxidized redox mediator at the counter-electrode, since dyes in the DSSCs are adsorbed as a mono-layer onto the mesoporous TiO$_2$ electrode [107]. Historically, ruthenium and volatile organic-based molecular sensitizers were used, but due to the presence of various pigments as well as environmental friendliness, which avoids the use of expensive rare metals with toxic volatile organics, much research work is now devoted to natural plant-based photosensitizers. Akin et al. [108] have designed and tested DSSCs sensitized by natural dyes having several pigments with various anchoring groups such as carbonyl, hydroxyl, and alkyl chains to clearly understand the photoinduced electron injection kinetics of these natural DSSCs. As a summary, the photoinduced electron transfer mechanism from plant extract photosensitizer is shown in Figure 12.
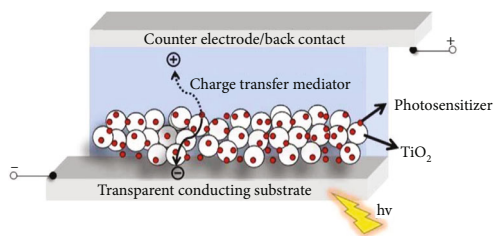
FIGURE 11: Configuration of a traditional dye-sensitized solar cell [107].

FIGURE 12: Photoinduced electron transfer mechanism in natural dye extracted plant [108].

5. Efficiency Optimization of Natural Plant Pigment-Based DSSCs

Ananthakumar et al. [70] showed that when a photoanode is functionalized by dyes containing organic dyes, it helps absorb more incident light. In order to increase the efficiency of solar cell devices further, the photoanode has been improved by low-cost transition metal oxide nanomaterials containing quantum dots. In addition, the cosensitization process also enhances light harvest efficiency. Thus, according to the review, 14% of efficiency was successfully reported. Hence, a sensitizer that is supported by a photoanode could successfully help to absorb visible light (enhance light harvesting capability) [109].

Al-alwani et al. [85] have optimized three different process parameters such as the nature of organic solvent based on their boiling point (ethanol, methanol, and acetonitrile), pH (4-8) and extraction temperature (50-90°C) for chlorophyll extraction from *Cordyline fruticosa* leaves by using response surface methodology. The optimal extraction conditions were a pH of 7.99, an extraction temperature of 78.33°C, and a solvent boiling point of 78°C. Therefore, at this optimal condition, the extracted pigment was used as a photosensitizer, and 0.5% of maximum solar conversion η was achieved [85]. Chien and Hsu [110] have reported an optimized anthocyanin photosensitizer extracted from red cabbage (*Brassica oleracea* var. *capitata f. rubra*), and best light-to-electricity conversion η was obtained when the pH and the concentration of the anthocyanin extract were at 8.0 and 3 mM, respectively, and when the immersion time for fabricating sensitized TiO_2 film was 15 min [111].

IK and Uthman [99] have reported an ethanol and distilled water-based extraction effect on doum palm fruit photosensitizer. From their report, the absorption transition between the dye ground state and excited states and the solar energy range absorbed by the dye are different. This difference is due to the existence of chromophores, which represent the chemical group that is responsible for the color of the molecule that is its ability to absorb photons. In detail, doum water extract has two absorption peaks at 350 nm and 400 nm, while the absorption peak of the doum ethanol extract adsorbed on TiO_2 was only at one absorption peak of 353 nm. It can be seen that after TiO_2 nanoparticles were added to doum pericarp extract, its absorption intensity decreased from 440 to 350 nm. Finally, the conversion efficiency for the ethanol extract was 0.012%, and water extract was up to 0.033% under the same light intensity [99].
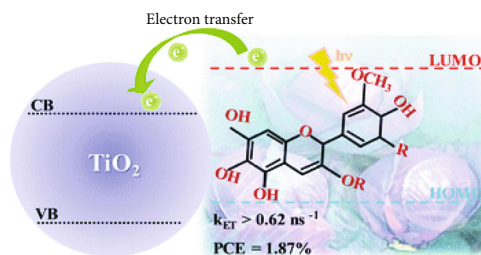
Gu et al. [8] have suggested that the absorption properties of natural dyes are strongly dependent on the types and concentration of pigments. According to their study, the photoelectric performance of different natural dyes from spinach, pitaya pericarp, orange peel, ginkgo leaf, purple cabbage, and carrot were measured as shown in Figure 13. They suggested that the V_{OC} of these dyes showed a similar value, corresponding to about 0.524 V, except for carrot, which showed only 0.276 V. The fill factors of these DSSCs are mostly higher than 0.5, which proves that a better conversion capability of photoelectric energy was obtained. For the short-circuit photocurrent density (J_{SC}), the values of these DSSCs based on different natural dyes are J_{SC} (purple cabbage) > J_{SC} (orange peel) > J_{SC} (spinach) > J_{SC} (ginkgo leaf) > J_{SC} (pitaya pericarp) > J_{SC} (carrot), and they arrive at 0.594, 0.325, 0.152, 0.111, 0.100, and 0.086 mA/cm^2, respectively. Meanwhile, the purple cabbage showed higher photoelectric conversion efficiency and reached 0.157% [8].

Optimization of the photoanode (TiO_2 nanostructure) is necessary for developing the high solar efficiency of DSSCs [74]. It is important that the thicker TiO_2 layers would also result in a dwindling transmittance and reduce the pigment dyes' absorption of light intensity. Also, the resistance to charge transfer might increase when the thickness of TiO_2 electrode layers increases [112]. García-Salinas and Ariza [113] have tried to optimize solvent extraction, method, pH, dye precursor, and dye extract stability. They focused on betalain pigments present in bougainvillea and beetroot extracts, and anthocyanins in eggplant extracts. Of these, beetroot extract showed 0.47% cell efficiency [113]. Later, they demonstrated improved power conversion of 1.3% by using roots of *Kniphofia schemperi* sensitizer in the presence of TiO_2 NPs biosynthesized in a (3:2) volume ratio due to effective surface modification, which enabled them to absorb an incident light [114, 115].

Norhisamudin et al. [116] have fabricated DSSCs using anthocyanin or chlorophyll natural dye extracts coming from Roselle (*Hibiscus sabdariffa*) and green tea leaves (*Camellia sinensis*). Both pigments were extracted using different alcohol-based solvents, namely, ethanol, methanol, and mixed (ethanol + methanol) to identify whether the different solvents had an effect during the dye extraction. According to their study, using a mixed solvent from methanol and ethanol and their mixture extraction system was done, and their mixture showed efficiency improvement. Thus, the comparison between Roselle (anthocyanin) dye

FIGURE 13: J-V curves for the DSSCs under standard simulated sunlight [8].
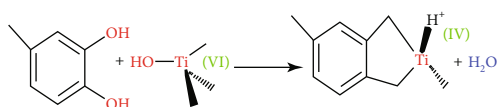
FIGURE 14: Chemical adsorption between TiO_2 films and effective groups [8].

extracts and green tea (chlorophyll) dye extracts shows that Roselle has higher efficiency and higher photosensitized performance.

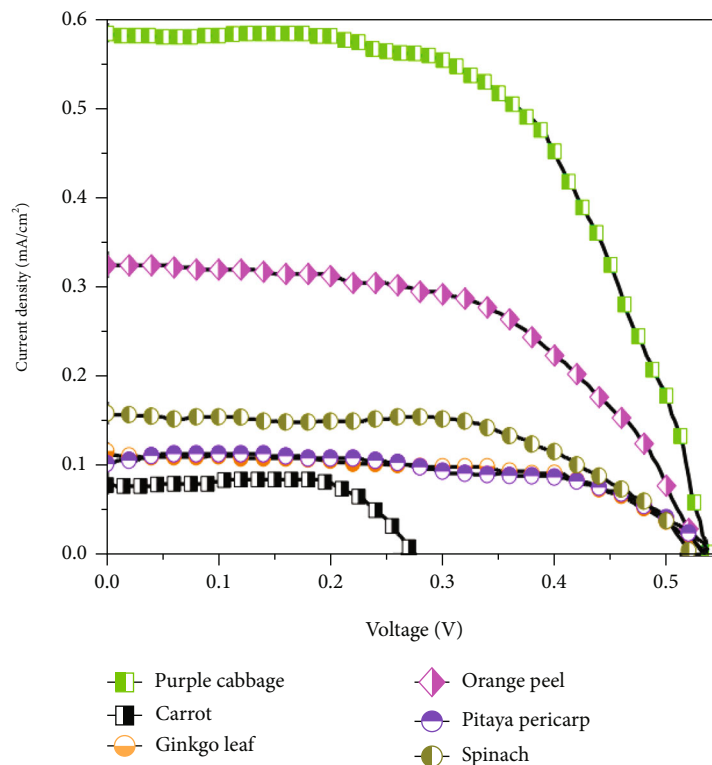Sensitization time and the number of natural dye coatings are the other big factors which affect DSSC performance. For example, in the betanin, indigo, and lawsone solar cells systems, 6, 12, 24, 36, and 48 hour sensitization times were tested. The time 24 hour was found to be an optimal time for sensitization in the case of betanin and lawsone solar cells, and 36 hour was observed to be optimum in the case of indigo solar cells. The optimal time of sensitization for the best performance of a particular dye is dependent on the rate of dye anchoring. lawsone and betanin have higher dipole moments, favoring the dipole-dipole interaction with TiO_2; moreover, they possess more favorable functional groups (-COOH and -OH) compared to indigo (with =CO groups), which will enable a higher rate of anchoring. Akin et al. reported the effects of anchoring groups on the photoinduced electron injection dynamics from natural dye molecules to TiO_2 nanoparticles. According to their report, nine different natural dyes having various anchoring groups were extracted from various plants and used as pho-

tosensitizers in DSSC applications. From these extracts, the long-hydroxyl and carbonyl-chain bearing anthocyanin, with the maximum electron transfer rate (k_{ET}), has shown the best photosensitization effect with regard to cell output. Despite the fact that their performance in DSSCs is somewhat lower or close to the metal complexes, these metal-free natural dyes can be treated as a new generation of sensitizers. It was reported that upon illumination, the dyes absorb light; an electron in a HOMO state is excited to LUMO state and further injected into a conduction band of TiO_2. Related to the physical adsorption, chemical adsorption is a more effective way to enhance the conversion efficiency, and usually, -OH, -COOH, C=O, $-SO_3H$, and $-PO_3H_2$ in the pigment were used as the effective groups and bonded with TiO_2, forming a chemical adsorption, just as shown in Figure 14. This action can facilitate the transfer of electrons from the dye to TiO_2. Therefore, according to Gu et al. report, the photoelectric conversion efficiency of dyes was η (purple cabbage) $> \eta$ (orange peel) $> \eta$ (spinach) $> \eta$ (pitaya pericarp) $> \eta$ (ginkgo leaf) $> \eta$ (carrot) and reached 0.157, 0.071, 0.054, 0.031, 0.030, and 0.010%, respectively, which is attributed to the synergistic reaction between the absorptive properties and molecular structure of natural dyes [8].

It is reported that the increase in the dye layer obstructs the charge transfer from the conduction band of the TiO_2 surface to the FTO electrolyte [69]. For the aforementioned reasons, the number of coatings in betanin-, indigo-, and lawsone-based solar cell configurations proved detrimental to the solar cell performance, possibly because of dye

(a)

(b)

FIGURE 15: Photovoltaic performance of spin-coated (blue dotted) and doctor blade-coated (red dotted) TiO_2 anodes photosensitized by jabuticaba fruit extract dye (a) a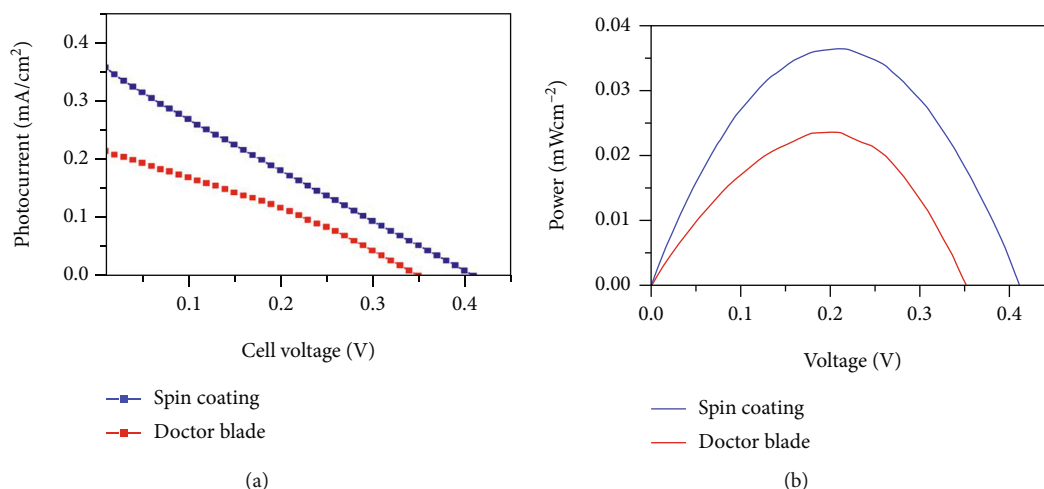nd power versus voltage curves of spin-coated (blue curve) and doctor blade-coated (red curve) TiO_2 thin films DSSCs using natural dyes extracted from the jabuticaba fruit (b) [100].

aggregation. In addition, doping agents are also the other factor which affects the efficiency of DSSCs in natural plant pigment containing dyes. For example, Bekele et al. [114] have reported that when TiO_2 nanoparticles are doped by Mg^{2+} ion and coated on an FTO glass substrate, they form Mg^{2+}-TiO_2-FTO photoanode. When this photoanode was immersed in methanol-extracted henna (*Lawsonia inermis*) leaf dye, its efficiency of light-to-electricity conversion was increased by generating the highest J_{sc}, from 0.66 to 1.28 ($mA\,cm^{-2}$), representing a 93% increase over the undoped TiO_2 group [117].

As seen from Figure 15(a), the short-circuit photocurrent density J_{SC} increases from 0.23 to 0.38 $mA\,cm^{-2}$ when the TiO_2 thin film is coated by the doctor blade and spin-coated techniques, respectively. The results indicate that the recombination rate increases in spin-coated TiO_2 thin film photoanodes. From the J-V curve, the highest values of J_{SC} and V_{OC} of the DSSCs were observed at 0.38 $mA\,cm^{-2}$ and 0.41 V, respectively. The maximum η obtained was 0.13% for spin-coated TiO_2 thin film electrodes and 0.08% for doctor blade method-coated electrodes. Figure 15(b) shows the power versus potential curves, and the corresponding power (P_{max}) obtained from spin-coated TiO_2 thin film DSSCs was 36.4 $\mu W\,cm^{-2}$, while the maximum power for the doctor blade method-coated electrode was 23.6 $\mu W\,cm^{-2}$ [100].

6. Computational Studies of Natural Plant Pigment-Based DSSCs

The computational calculation principle on extracts from natural plant-based pigments has provided a valuable reference for predicting precise protocols about the structure and photoelectrical property relationships between molecules using the Gaussian 09 package. The model enabled to identify essential electronic and structural attributes that quantify the molecular prerequisites of certain classes found in

the natural dye, which are responsible for high power conversion efficiency for DSSCs [118, 119].

In detail, the dye structure properties' ground state could be optimized using DFT with the B3LYP functional at a 6-31G(d) basis set, while excited states were calculated using TD-DFT with different functionals, including Cam-B3LYP, MPW1PW91, and PBEPBE, at the same basis set calculation method [92]. To clarify this, Maahury and Martoprawiro [120] have studied the computational calculations of anthocyanin, which is evaluated as a basic reference biomolecule and used as the main photosensitizer in DSSCs [83]. Their geometry optimization calculations showed that the structures of anthocyanin compounds are not planar and their single point calculations for excited states showed that their absorption wavelength was shorter than experimental data (i.e., its difference was between 7.3% and 8.3%). The calculations were computed by DFT with B3LYP functional and 6-31G (d) for ground state optimization and TD-DFT for excited states based on a single point calculation system [120].

Ghann et al. [98] reported that the computational calculation on delphinidin, which is an anthocyanin derivative that is found in pomegranate fruit, resulted in HOMO and LUMO values of -8.71 eV and -6.27, respectively. This makes effective electron transfer of charge possible from the LUMO of the pigment into the conduction band of TiO_2. To support this, the HOMO and LUMO surfaces and their orbital energy diagrams are shown in Figures 16(b) and 16(c), respectively. For this electron transfer, the blue and red regions represented the positive and negative values of the orbitals, respectively. The regeneration of the dye caused by the redox electrolyte (I^-/I_3^-) coupling increases the lifetime of the dye itself. Also, the narrower band gap of delphinidin dye, with a value of 2.44 eV, increases the intramolecular electronic transition probabilities [98]. From these and other literature studies, it is summarized that the electronic transition computational protocols are composed of six main steps. These are (i) engineering band gaps, (ii)
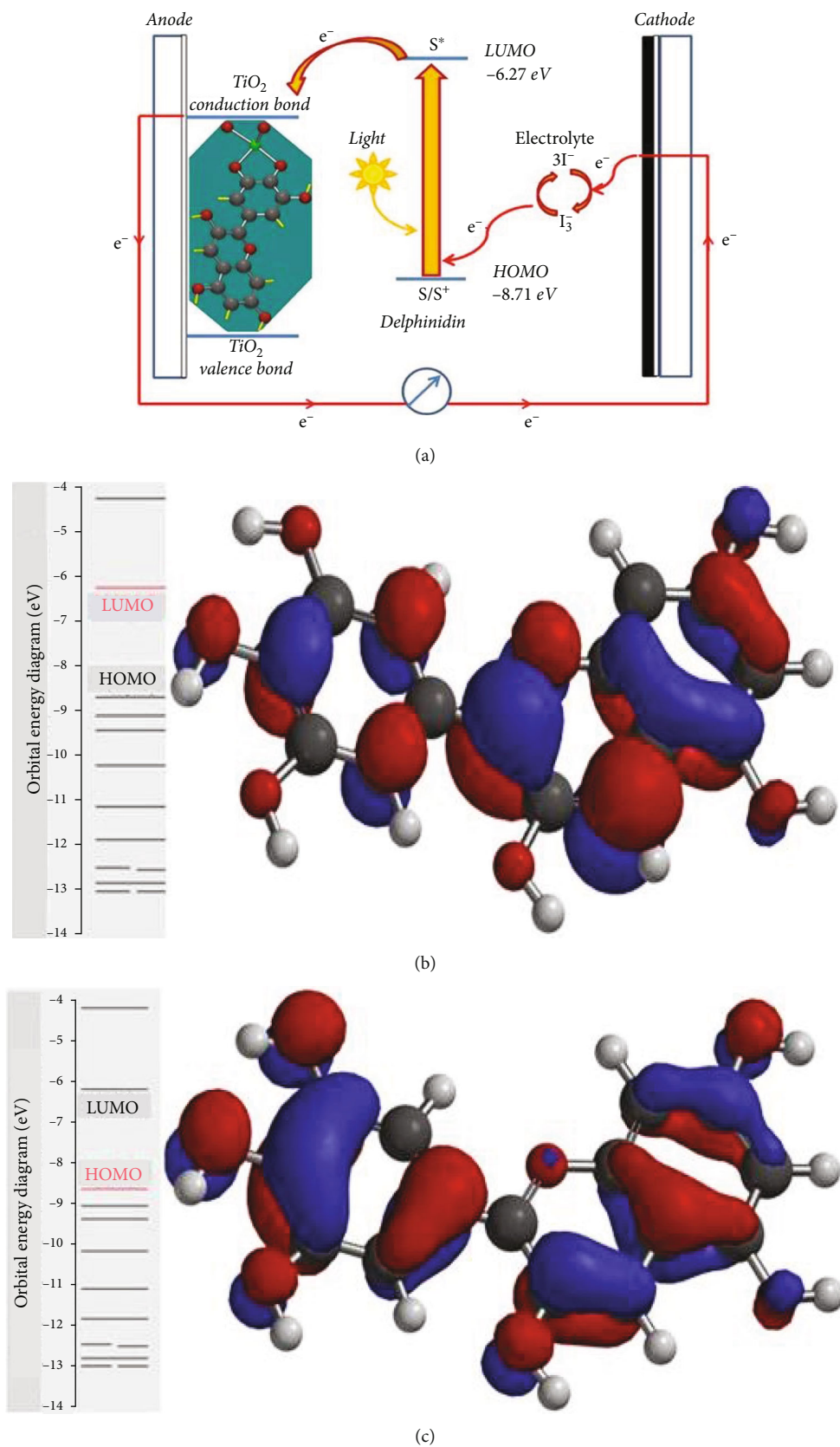
(a)

(b)

(c)

Figure 16: Working principles of DSSCs with delphinidin (a), LUMO (b), and HOMO surface and orbital energy diagram for delphinidin (c) [98].
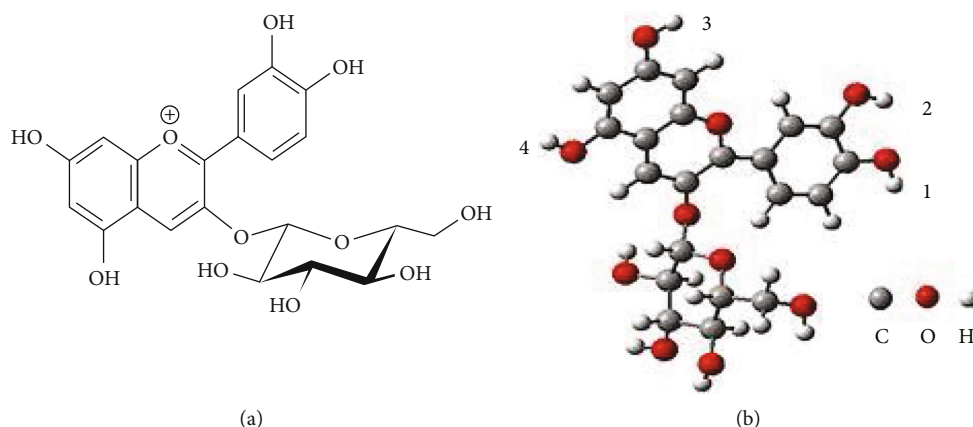
(a) (b)

FIGURE 17: Cyanidin 3-glucoside structure (a) and labeling of the deprotonation sites (b) [122].

photoabsorption spectrum of dyes, (iii) adsorbed dyes onto the anode surface, (iv) short-circuit current density, J_{SC}, (v) open-circuit photovoltage, V_{OC}, and (vi) photocurrent-photovoltage curve, and fill factor, FF [121]. Based on this fact and for simplicity, Mohankumar et al. [119] explained that twelve novel dye molecules developed from D-π-A-based triphenylamine (TPA) were studied to evaluate their suitability for applications in DSSCs by using DFT and TD-DFT. The optimization effects of flavone and isoflavone on TPA-based dyes were successfully studied using B3LYP and CAM-B3LYP density functionals combined with 6-311G (d, p) basis set in their computational study.

Ndiaye et al. [122] studied the experimental and computational behavior of chrysanthemin (cyanidin 3-glucoside) pigment in DSSCs. Its theoretical study of chrysanthemin was performed with the GAUSSSIAN 09 simulation. A better energy level alignment was found for partially deprotonated molecules of chrysanthemin, with the excited photoelectron having enough energy in order to be transferred to the conduction band of TiO$_2$ semiconductor in DSSCs. Experimentally, an aqueous extract of Roselle (*Hibiscus sabdariffa*) calyces was considered as the source of chrysanthemin, and the extracts having various pH values were tested in DSSCs. The detailed analysis of HOMO and LUMO of the cyaniding 3-glucoside molecule deprotonated in positions 1, 2, 3, bound to the TiO$_2$ surface shows a large electron density on the deprotonated anchor groups, which favors the electron transfer from the excited molecule to the semiconductor as shown in Figure 17 [122].

The analysis of the molecular orbitals showed that the probability distribution of electron density at the HOMO and LUMO levels is predominantly around the NH and C=O groups in the molecule. The two nonbonding electrons on the N atom participate in the delocalization of the π-electrons of the conjugated systems that correspond to the HOMO energy levels (see Figure 18(a)) and the antibonding $\pi *$ orbitals arise from the LUMO level of indigo as shown in Figure 18(b). The photoexcitation of the nonbonding electrons coming from the electron donor NH group to the antibonding $\pi *$ orbital in the electron acceptor C=O group forms the $n \longrightarrow \pi *$ electronic transitions. The C=O group

helps the pigment anchor with TiO$_2$. The electron density map that is shown in Figure 18(c) indicates the distribution of charge on the indigo molecule (green and red colors represent electropositivity and electronegativity, respectively). As the molecule is symmetric, the net dipole moment is negligible and is equal to 0.0053 D [69]. It is known that hypericin is a naphthodianthrone, a red-colored anthraquinone derivative, a photosensitive pigment, which is one of the principal active constituents of St. John's wort (*Hypericum perforatum*). As a result, this pigment exhibited good adsorption onto a semiconductor surface, a high molar absorption coefficient (43700 L mol^{-1} cm^{-1}) and favorable alignment of energy levels and provided a long lifetime of electrons (17.8 ms) on the TiO$_2$ photoanode surface [123].

The probability distribution of the electron density corresponding to the HOMO and LUMO levels are located to both benzoid and quinoid moieties, respectively (Figures 18(d) and 18(e)). The first absorption peak at 338 nm is primarily caused by HOMO to LUMO transitions within the C=C ($\pi \longrightarrow \pi *$) and C=O ($n \longrightarrow \pi *$) regions of the lawsone quinoidal ring. The absorption peak seen in the visible region at 410 nm arises from the $n \longrightarrow \pi *$ transitions localized mainly around the oxygen atom of the quinoidal ring. So, Figure 18(f) shows the distribution of charge on the lawsone molecule. From this pigment, the carbonyl carbons of C=O groups could be observed to be highly electropositive, showing a net dipole moment equal to 5.78 D, indicating the strong electron-withdrawing nature of the C=O group anchors the lawsone molecule onto TiO$_2$ [69].

Cosensitizing pigments with a complementary absorption spectra increase the absorption band and are an attractive pathway to enhance the efficiency in DSSCs [124]. Ramirez-Perez et al. [104] reported that the predominance of hydroxyl groups on the aromatic skeleton of anthocyanin gives rise to an intense blue color, while a red color is observed in methoxyl functional groups [104]. In brief, lawsone solar cells displayed better performance, showing average efficiencies of $0.311 \pm 0.034\%$, compared to indigo solar cells showing efficiencies of $0.060 \pm 0.004\%$. So, the betanin/lawsone cosensitized solar cell reflected a higher average efficiency of $0.793 \pm 0.021\%$ as compared to the $0.655 \pm 0.019\%$

(a)

(b)

(c)

(d)

(e)

(f)
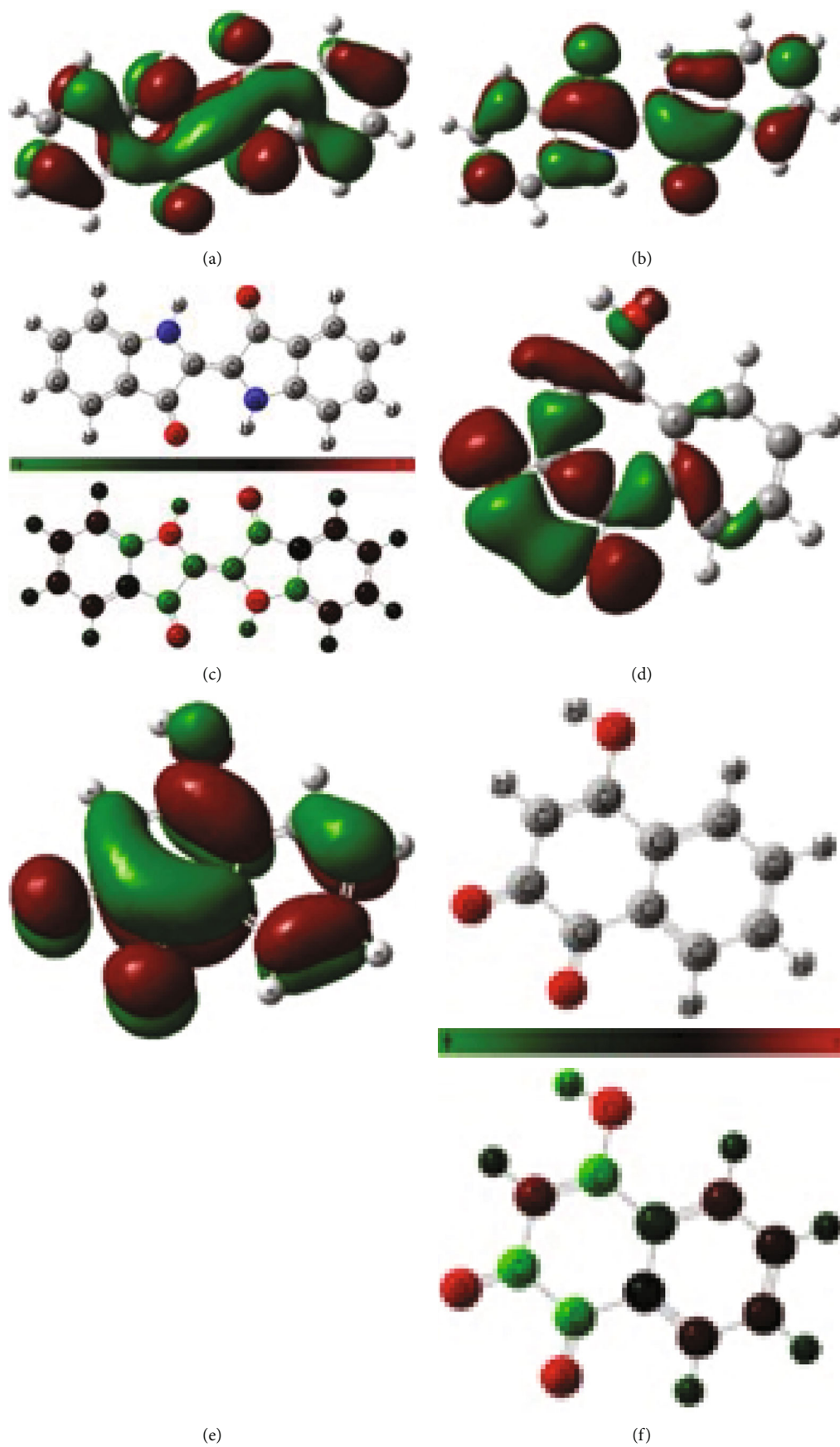
FIGURE 18: Continued.
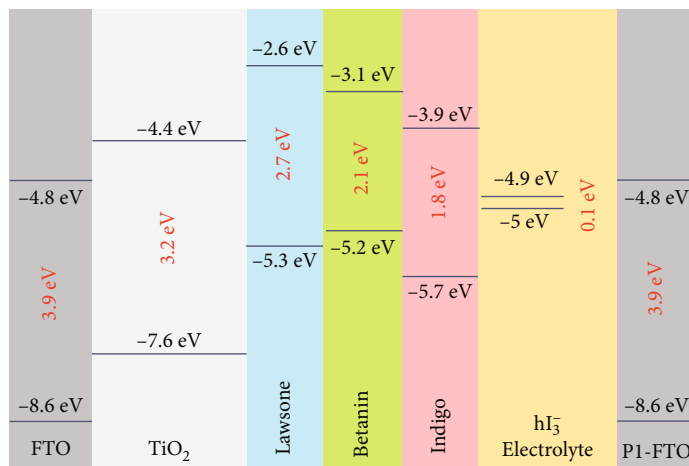
(g)

FIGURE 18: Electron density corresponding to the HOMO energy level (a), LUMO energy level (b), and charge distributions of indigo (c). Electron density corresponding to the HOMO energy level (d), LUMO energy level (e), charge distributions of lawsone (f), and alignment of the energy levels (with respect to vacuum) of the materials with respect to each other (g) [69].
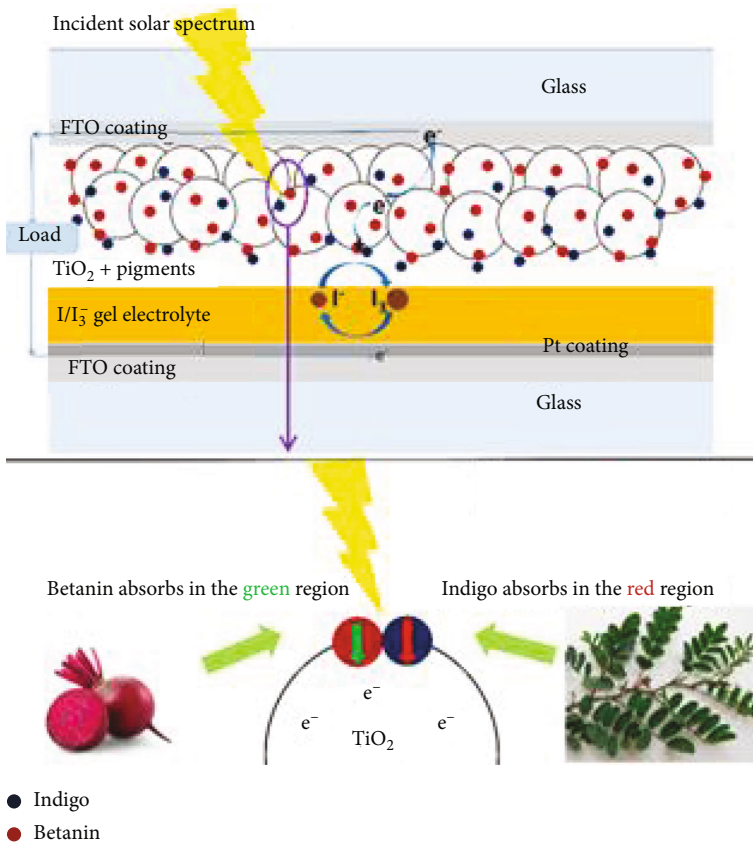
(a)

FIGURE 19: Continued.

(b)
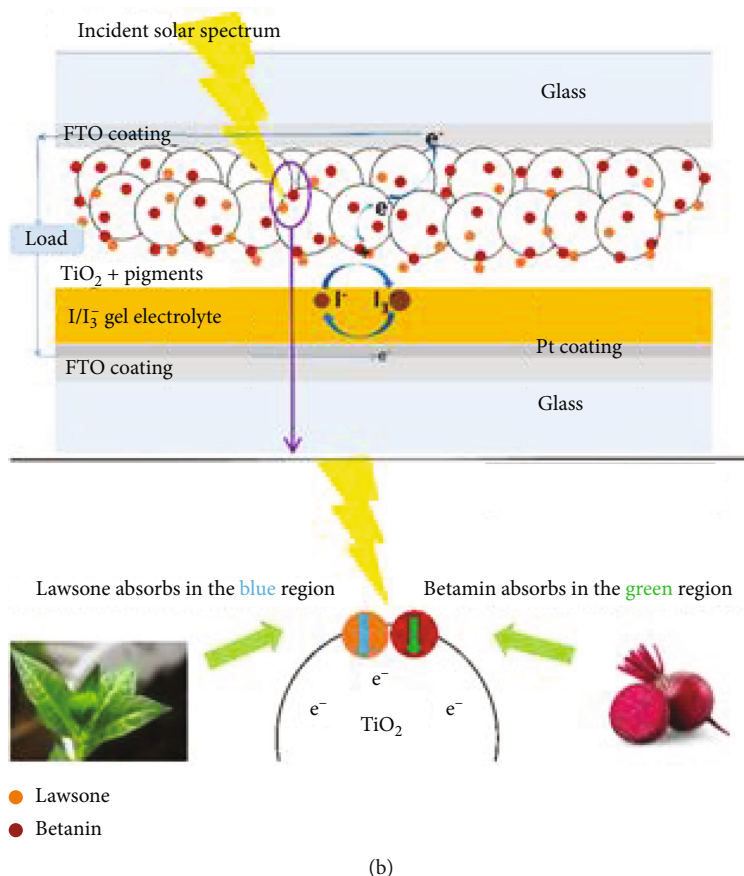
FIGURE 19: Illustration of the device showing the complementary absorption by the cosensitized pigments of betanin and indigo (a) and betanin and lawsone (b) [69].

(a)   (b)
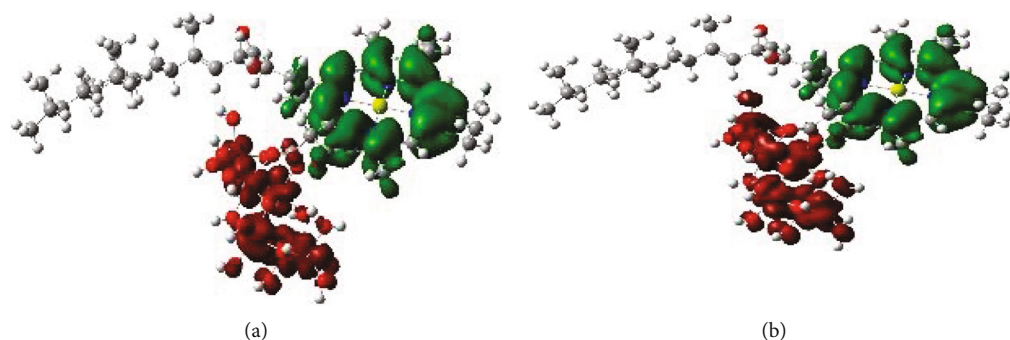
FIGURE 20: Charge difference density (CDD) for chlorophyll/TiO$_2$. S6 (a) and S9 (b) [92].

obtained for the betanin/indigo cosensitized solar cell. An 11.7% enhancement in efficiency (with respect to betanin) was observed for the betanin/indigo solar cell, whereas a higher enhancement of 25.5% was observed for the betanin/lawsone solar cell. Impedance spectroscopy improved that the higher efficiency can be attributed to the higher electron lifetime of 313.8 ms in the betanin/lawsone cosensitized solar cell compared to 291.4 ms in the betanin/indigo solar cell (Figure 19) [69].

The computational analysis and experimental verification of photosensitizers and their efficiency performances done by Liu et al. [92] have reported that the simulated

absorption spectra of chlorophyll were extracted from six different leaves by using ethanol solvent. To compare with the experimental results, the excited state properties of chlorophyll was investigated via the TD-DFT method with different functionals at a 6-31G(d) basis set based on the optimized ground state structure of chlorophyll. The choice of chlorophyll pigment was due to the fact that it accounts for the largest proportion of the green plant leaves. The charge different density results showed the distribution of charge during the light absorption step (Figure 20). As stated, for the sixth excited state, a red electron is moved into the semiconductor, and a hole is resided in the porphyrin

(a)

(b)

(c)
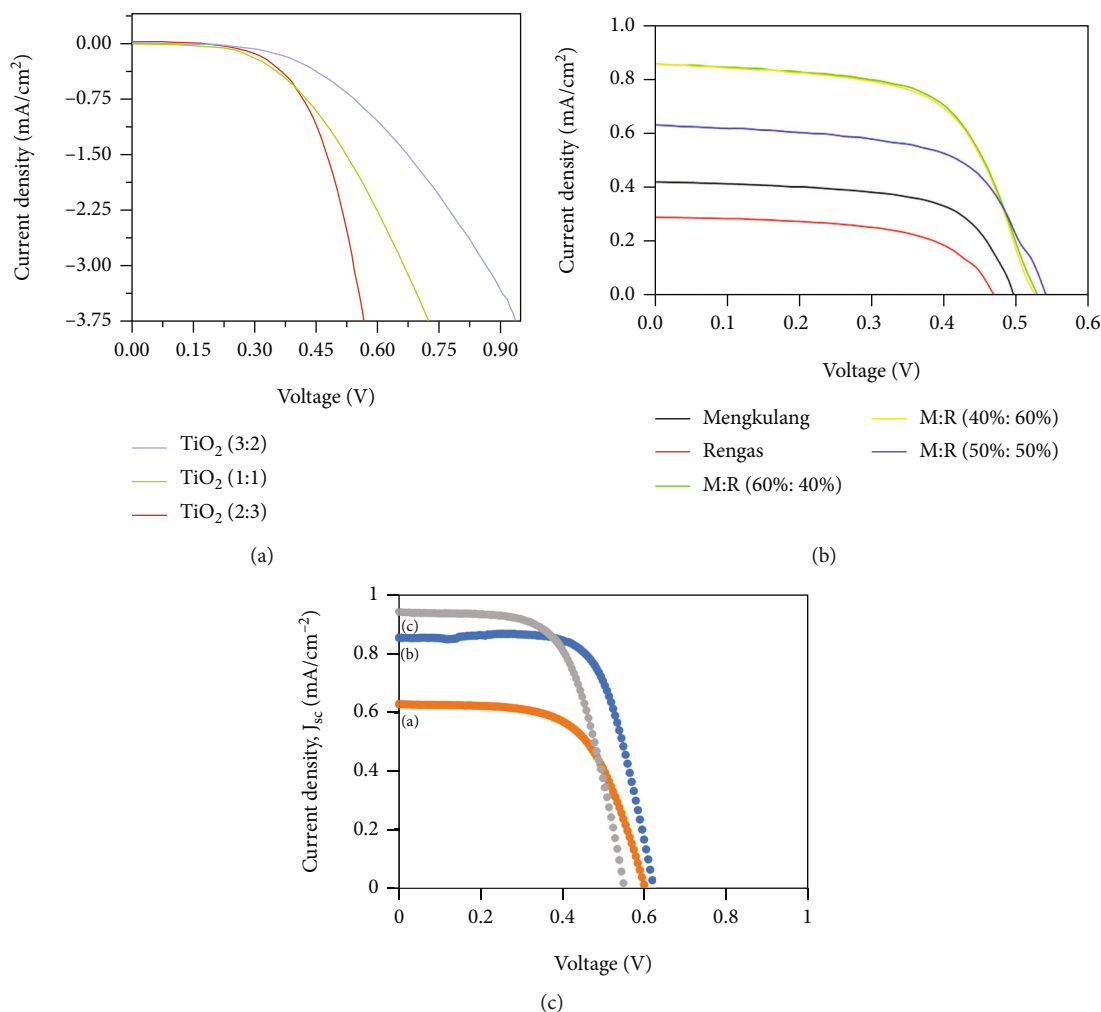
FIGURE 21: J-V curve of root extract of *Kniphofia schemperi* (a), mengkulang and rengas wood and their mixed sensitizers (b), and different cells at different solvents (c) [methanol (i), ethanol (ii), and acetone (iii)] extracted from *Costus woodsonii* leaves [78, 114, 133].

ring. Previously, chlorophyll, natural porphyrin, and its derivatives have been studied using DFT approaches to explore their spectroscopic properties and their future applications in DSSCs [125]. As a result, this state is a charge transfer (CT) state, and a similar CT process can be found in the ninth excited state, where more electron migration into the semiconductor benefits electron transport for external circuit. The calculated excitation energies (E, eV), for the sixth excited state (S6) and the ninth excited state (S9) were 2.6161 eV and 2.9989 eV, respectively. This confirmed the existence of electron transfer into the semiconductor during photoexcitation.

As a summary, both experimental and computational modeling (relative energy calculations of HOMO and LUMO of natural plant pigment extraction) allowed electron injection ability elucidation of the extracted plant pigments [126]. These investigations, when the natural plant pigments are highly aggregated on the TiO_2 surface, affects the DSSCs' performance [127, 128].

7. Performance Characterization Parameters in DSSCs

7.1. Characterization Using Photocurrent Density-Voltage (J-V). The general performance of the assembled DSSCs prepared using their components could be evaluated by different parameters such as J_{SC}, η, V_{max}, P_{max}, V_{OC}, and FF. Bekele et al. [114] reported on synthesis of TiO_2 nanoparticles within three different volume ratios as $2:3$, $1:1$, and $3:2$ in the presence of *Kniphofia schemperi* root ethanol extract both as a capping and reducing agent and also as a natural sensitizer. Synthesized $2:3$, $1:1$, and $3:2$ photoelectrodes show V_{OC} performance of 63, 48, and 161 mV, respectively. The $3:2$ photoelectrode shows best V_{OC} as compared to the remaining electrodes, and this improvement could be attributed to the improved absorption of light in the presence of *Kniphofia schemperi* root sensitizer, and this is due to the more improved surface morphology of the photoelectrode. This photoelectrode provides enhanced efficiency ($\approx$1.30%)

(a)

- ●— TiO_2 (2:3)
- ●— TiO_2 (3:2)
- ●— TiO_2 (1:1)
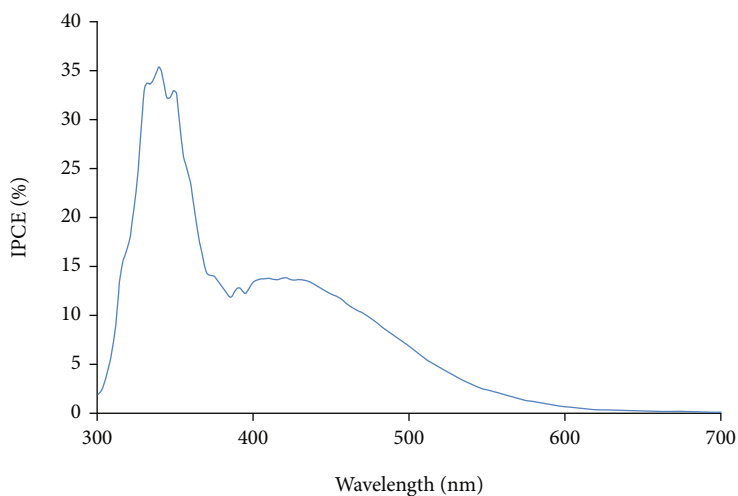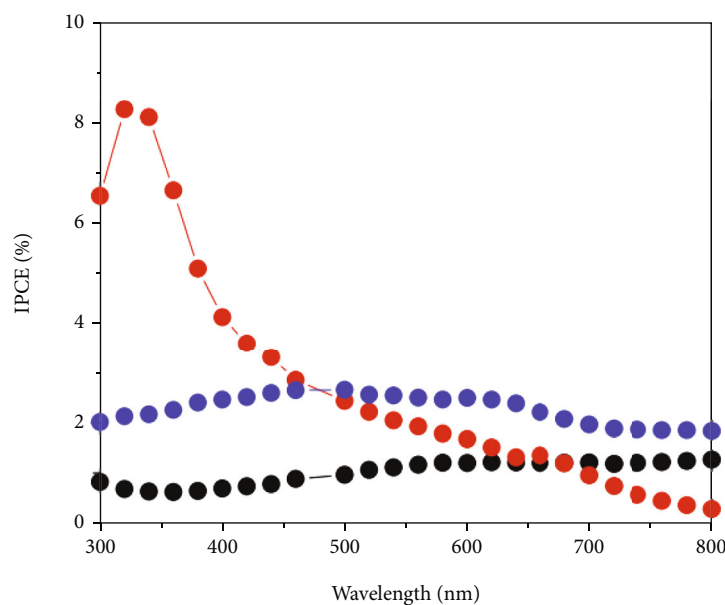
(b)

FIGURE 22: IPEC% curve of *Pandannus amaryllifolius* leaves (a) and root extract of *Kniphofia foliosa* (b)-based DSSCs [114, 134].

as compared to the remaining ratio photoelectrode due to its small average crystalline size, which enables it to adsorb excess dye molecules on its surface [129]. The corresponding J_{SC} and FF values for each of the different volume ratios of TiO_2 photoelectrode-based DSSCs were estimated as 1.29×10^{-3}, 6.05×10^{-3}, and 2.46×10^{-2} mA/cm^2, and the resultant FF was 42, 40.3, and 32.8% for the TiO_2 (2:3), TiO_2 (1:1), and TiO_2 (3:2) photoelectrodes, respectively. TiO_2 (3:2) outperforms the other two green prepared photoelectrodes due to the better catalytic property of the photoelectrode, which was achieved by using less extract during synthesis.

Senthamarai et al. [82] reported on the green synthesis of TiO_2 nanostructure photoelectrodes prepared *via* the green route using the fruit extracts of pineapple, orange, and grapes as reducing and stabilizing agents, for DSSC application in the presence of fruit skin ethanol extract of *Murraya koenigii* sensitizer. The grape-mediated synthesized TiO_2 photoelectrode shows the maximum solar cell efficiency (1.78%). In the presence of *Murraya koenigii* natural sensitizer, pineapple-templated TiO_2 and orange-templated TiO_2 photoelectrodes shows solar cell efficiency of 1.61% and 1.52%, respectively, in the presence of fruit skin extract. The corresponding V_{OC} values for the grape-TiO_2, orange-

TiO_2, and pineapple-TiO_2 photoelectrodes were found to be 0.628, 0.626, and 0.576 mV, respectively.

Moreover, reports show that ZnO-TiO_2-Fe_2O_3 nano-composites were synthesized and used as an alternative photoelectrode in the presence of ethanol-extracted *Guizotia scabra* and *Salvia leucanta* flower sensitizers [130]. It has been found that the obtained conversion efficiencies for the ethanol extracts of *Guizotia scabra* and *Salvia leucantha* were estimated at 0.0013% and 0.0017%, respectively. According to Cho et al. [131], the ethanol extract of the mixed sweet potato leaf and blueberry sensitizer at a weight concentration of 40% (1 : 1) volume ratio was used to coat the TiO_2 photoanode, and the report shows that 0.61 V, 4.75 mA/cm^2, 53%, and 1.57% of V_{OC}, J_{SC}, FF, and η were achieved, respectively. But the individual single sensitizers of sweet potato leaf sensitizer show 0.645 V, 1.23 mA/cm^2, 49%, and 0.391%, and blueberry flower sensitizer-based DSSCs provide 0.67 V, 0.532 mA/cm^2, 61%, and 0.218% of V_{OC}, J_{SC}, FF, and, η, respectively.

Safie et al. [78] reported on the use of mengkulang and rengas wood and their mixed ratios (60 : 40, 40 : 60, and 50 : 50) in the presence of TiO_2 nanoparticle photoelectrode. The report proves that the cell performance was found to be 0.53 V, 0.40 mA/cm^2, 75.98%, 0.16%, and 0.50 V, 0.30 mA/cm^2, 72.88%, and 0.11% of V_{OC}, J_{SC}, FF, and η for the mengkulang and rengas wood sensitizer-based DSSCs, respectively, while the different mixed ratios of those sensitizers based on DSSC performance were found to be 0.54 V, 0.60 mA/cm^2, 63.28%, 0.21%, 0.53 V, 0.90 mA/cm^2, 61.78%, 0.29%, 0.53 V, 0.90 mA/cm^2, 62.16%, and 0.30% for the 50 : 50, 40 : 60, and 60 : 40 volume ratios of mengkulang and rengas wood sensitizer, respectively. Figures 21(a)–21(c) display the effect of the photoelectrode on the performance of the photovoltaic parameters of DSSCs. Figure 21(b) depicts the J-V curve of green synthesized TiO_2 NP photoelectrode within different volume ratio-based DSSCs in the presence of ethanolic root extract of *Kniphofia schemperi*, while Figure 21(c) shows the J-V curve of mengkulang and rengas wood and their mixed sensitizers in the presence of TiO_2 nanostructured photoanode. When TiO_2 nanoparticles are layered with graphitic carbon nitride structure by forming composites, it decreases the energy barrier of electron transport and improves the injection efficiency of photogenerated electrons from the photoanode [132].

Najihah and Tan [133] designed and reported on the methanol, ethanol, and acetone extracted from *Costus woodsonii* leaves as a natural sensitizer for DSSCs. It has been found that the short circuit current density, open circuit voltage, fill factor, and efficiency of methanol-extracted *Costus Woodsonii* leave sensitizer-based DSSCs shows 0.63, 0.60, 0.61, and 0.23, respectively. The ethanol-extracted *Costus woodsonii* leave sensitizer-based DSSCs are 0.85, 0.63, 0.69, and 0.37, respectively. In addition, as can be seen in Figure 21(c), acetone-extractable sensitizer shows 1.35, 0.57, 0.62, and 0.48, respectively, which is the best performing solvent. The report proves the effect of the solvent and, in turn, its influence on the performance of the various photovoltaic parameters. The light absorption capability of the sensitizer-coated photoelectrode is directly correlated to the concentration of the natural dye in an extraction solvent [78, 133]. Among the three solvents, acetone-extracted sensitizer-based DSSCs provide better efficiency relative to the corresponding counterparts.

7.2. Characterization Using Incident Photon to Current Conversion Efficiency (IPCE). The IPCE, also known as the external quantum efficiency, is the percentage of incident photons converted to electric current (collected charge carriers) when the device is operated in a short circuit. As reported by Al-Alwani et al. [134], the incident photon to current conversion efficiency of DSSCs is found to be dependent on the nature of the photoanode and also the light absorption and capacity behavior of natural sensitizers, as shown in Figures 22(a) and 22(b). As supported in Figure 22(b), the IPCE value of *Kniphofia foliosa* ethanolic root extract in the presence of various volume ratios (2 : 3, 1 : 1, and 3 : 2) of green-synthesized TiO_2 photoelectrode was found to be altered with the variation in the volume ratio of the photoanode. As could be provided in Figure 22(b), relatively maximum IPCE% ($\approx$8.11%) value was obtained in the presence of TiO_2 photoelectrode formed within the volume ratio of 3 : 2 and was located at a wavelength scan of 340 nm, while the TiO_2 (1 : 1) photoelectrode provides an IPCE of 2.66%, which occurs at around 500 nm.

DSSC is an efficient photovoltaic technology in wireless sensors and indoor light due to its low cost and material abundancy in nature. However, Kokkonen et al. [32] have reviewed the possible scaling up of fabrication methods at industrial manufacturing level for high-performance stability and high photovoltaic efficiency under typical indoor conditions. Hence, a significant research effort has been invested in exploring the new generation of photovoltaic devices as alternatives to traditional silicon- (Si-) based solar cells [135]. Moreover, the efficiency and its research challenges towards DSSCs have been clearly reviewed [136]. To solve such problems, recently, the discovery of new materials, such as 2D and high selectivity catalysts, have been emerged as promising materials, and their identifications have been identified by machine learning data-driven approach [137]. Especially, indoor solar cell is a strong positive influence on the ecology of the Internet of Things (IoTs). This IoT contained communication devices, actuators, remote, and distributed sensors. Particularly, smart IoT sensors have the potential of performing control functions and mass monitoring, which is driven by an indoor power gathering system [138, 139].

8. Conclusion and Future Outlook

8.1. Conclusion. It has been observed from the review work that DSSCs and their various components were fabricated *via* different protocols. The CE and the photoanode of DSSCs were fabricated *via* various chemical and green methods. It has been observed that even if the electrodes of DSSCs prepared *via* chemical methods were to provide efficient efficiency as compared to the electrodes prepared *via*

green method, the electrodes fabricated *via* green technique is found to be cost effective, environmentally friendly, and also able to provide a high surface area to volume ration, which makes them available for harvesting much of the sun's light on their surface. Using numerous green and medicinal parts of natural plants such as leaves, roots, steams, barks, flowers, and other medicinal green plants as photosensitizers is the most preferable option.

8.2. Future Outlook. In order to achieve the real utilization of natural pigment-based conversion of solar light energy to electricity in the near future, the scientific community should be addressing and solving the problem of the less efficient properties of DSSCs. This could be possible by improving the major components of the device *via* numerous modification protocols. In order to articulate a best-performing device and enhance the efficiency, the device must be assembled by considering those parameters. This enables the device to achieve enhanced cell performance and efficiency.

Conflicts of Interest

There is no conflict of interest between authors.

Authors' Contributions

The authors contributed equally to this work.

Acknowledgments

References

[1] A. Y. Al-Baitai and F. M. Ibrahim, "Dye sensitized solar cells based on natural dye-a review," *International Research Journal of Innovations in Engineering and Technology*, vol. 6, no. 1, pp. 48–53, 2022.

[2] M. A. Majid, "Renewable energy for sustainable development in India: current status, future prospects, challenges, employment, and investment opportunities," *Energy, Sustainability and Society*, vol. 10, no. 1, pp. 1–36, 2020.

[3] G. Beaudoin, D. Robertson, R. Doherty, D. Corren, B. Staby, and L. Meyer, "Technological challenges to commercial-scale application of marine renewables," *Oceanography*, vol. 23, no. 2, pp. 32–41, 2010.

[4] M. S. Ahmad, A. K. Pandey, and R. N. Abd, "Advancements in the development of TiO_2 photoanodes and its fabrication methods for dye sensitized solar cell (DSSC) applications. A review," *Renewable and Sustainable Energy Reviews*, vol. 77, no. 77, pp. 89–108, 2017.

[5] A. Andualem and S. Demiss, "Review on dye-sensitized solar cells (DSSCs)," *Edelweiss Applied Science and Technology*, no. 2, pp. 145–150, 2018.

[6] F. Martins, C. Felgueiras, and M. Smitková, "Fossil fuel energy consumption in European countries," *Energy Procedia*, vol. 153, pp. 107–111, 2018.

[7] G. Richhariya, A. Kumar, P. Tekasakul, and B. Gupta, "Natural dyes for dye sensitized solar cell: A review," *Renewable and Sustainable Energy Reviews*, vol. 69, no. 69, pp. 705–718, 2017.

[8] P. Gu, D. Yang, X. Zhu, H. Sun, and J. Li, "Performance of dye-sensitized solar cells based on natural dyes," *Optical and Quantum Electronics*, vol. 50, no. 5, pp. 1–3, 2018.

[9] S. N. Karthick, K. V. Hemalatha, S. K. Balasingam, F. Manik Clinton, S. Akshaya, and H. J. Kim, "Dye-sensitized solar cells: history, components, configuration, and working principle," *Interfacial Engineering in Functional Materials for Dye-Sensitized Solar Cells*, vol. 5, pp. 1–6, 2019.

[10] R. Singh, "Dye-sensitized solar cell technology: recent development and advancement," in *Green Energy and Technology*, A. Sharma, A. Shukla, and L. Aye, Eds., pp. 221–250, Springer Singapore, Singapore, 2018.

[11] I. Joseph, H. Louis, T. O. Unimuke, I. S. Etim, M. M. Orosun, and J. Odey, "An Overview of the Operational Principles, Light Harvesting and Trapping Technologies, and Recent Advances of the Dye Sensitized Solar Cells (Review)," *Applied Solar Energy*, vol. 56, no. 5, pp. 334–363, 2020.

[12] K. Zeng, Z. Tong, L. Ma et al., "Molecular engineering strategies for fabricating efficient porphyrin-based dye-sensitized solar cells," *Energy & Environmental Science*, vol. 13, no. 6, pp. 1617–1657, 2020.

[13] N. Edomah, "Economics of energy supply," in *Reference Module in Earth Systems and Environmental Sciences*, pp. 1–16, Elsevier, 2018.

[14] M. Giannouli, "Current status of emerging PV technologies: a comparative study of dye-sensitized, organic, and perovskite solar cells," *International Journal of Photoenergy*, vol. 2021, Article ID 6692858, 19 pages, 2021.

[15] V. Venkatraman, R. Raju, S. P. Oikonomopoulos, and B. K. Alsberg, "The dye-sensitized solar cell database," *Journal of Cheminformatics*, vol. 10, no. 1, article 18, 2018.

[16] H. Bourdoucen, J. A. Jervase, A. Al-Badi, A. Gastli, and A. Malik, "Photovoltaic cells and systems: current state and future trends," *Sultan Qaboos University Journal for Science [SQUJS]*, vol. 1, no. 5, pp. 185–207, 2017.

[17] S. Sharma, K. K. Jain, and A. Sharma, "Solar cells: in research and applications—a review," *Materials Sciences and Applications*, vol. 6, no. 12, pp. 1145–1155, 2015.

[18] Y. Kusumawati, A. S. Hutama, D. V. Wellia, and R. Subagyo, "Natural resources for dye-sensitized solar cells," *Heliyon*, vol. 7, no. 12, article e08436, 2021.

[19] B. O'Regan and M. Grätzel, "A low-cost, high-efficiency solar cell based on dye-sensitized colloidal TiO_2 films," *Nature*, vol. 353, no. 6346, pp. 737–740, 1991.

[20] K. Sharma, V. Sharma, and S. S. Sharma, "Dye-sensitized solar cells: fundamentals and current status," *Nanoscale research letters*, vol. 13, no. 1, pp. 1–46, 2018.

[21] S. Arunmetha, V. Rajendran, M. Vinoth et al., "An efficient photoanode for dye sensitized solar cells using naturally derived S/TiO_2 nanoparticles," *Materials Research Express*, vol. 4, no. 3, article 035016, 2017.

[22] A. Carella, F. Borbone, and R. Centore, "Research progress on photosensitizers for DSSC," *Frontiers in chemistry*, vol. 6, no. 6, p. 481, 2018.

[23] X. Guo, G. Lu, and J. Chen, "Graphene-based materials for photoanodes in dye-sensitized solar cells," *Frontiers in Energy Research*, vol. 14, no. 3, p. 50, 2015.

[24] M. Giannouli, K. Govatsi, G. Syrrokostas, S. N. Yannopoulos, and G. Leftheriotis, "Factors affecting the power conversion

efficiency in ZnO DSSCs: Nanowire vs. nanoparticles," *Materials*, vol. 11, no. 3, p. 411, 2018.

[25] M. E. Ragoussi and T. Torres, "New generation solar cells: concepts, trends and perspectives," *Chemical Communications*, vol. 51, no. 19, pp. 3957–3972, 2015.

[26] A. M. Ammar, H. S. H. Mohamed, M. M. K. Yousef, G. M. Abdel-Hafez, A. S. Hassanien, and A. S. G. Khalil, "Dye-sensitized solar cells (DSSCs) based on extracted natural dyes," *Journal of Nanomaterials*, vol. 2019, Article ID 1867271, 10 pages, 2019.

[27] K. Ebrahim, "Dye Sensitized Solar Cells-Working Principles, Challenges and Opportunities," in *Solar Cells-Dye-Sensitized Devices*, vol. 8, InTech, 2011.

[28] G. Zhang, G. Kim, and W. Choi, "Visible light driven photocatalysis mediated via ligand-to-metal charge transfer (LMCT): an alternative approach to solar activation of titania," *Energy & Environmental Science*, vol. 7, no. 3, pp. 954–966, 2014.

[29] F. Bella, C. Gerbaldi, C. Barolo, and M. Grätzel, "Aqueous dye-sensitized solar cells," *Chemical Society Reviews*, vol. 44, no. 11, pp. 3431–3473, 2015.

[30] N. T. Kumara, A. Lim, C. M. Lim, M. I. Petra, and P. Ekanayake, "Recent progress and utilization of natural pigments in dye sensitized solar cells: A review," *Renewable and Sustainable Energy Reviews*, vol. 78, no. 78, pp. 301–317, 2017.

[31] A. D. Marques, V. A. da Silva, E. S. Ribeiro, and L. F. Malta, "Dye-sensitized solar cells: components screening for glass substrate, counter-electrode, photoanode and electrolyte," *Materials Research*, vol. 23, p. 23, 2020.

[32] M. Kokkonen, P. Talebi, J. Zhou et al., "Advanced research trends in dye-sensitized solar cells," *Journal of Materials Chemistry A*, vol. 9, no. 17, pp. 10527–10545, 2021.

[33] D. Devadiga, M. Selvakumar, P. Shetty, and M. S. Santosh, "Dye-sensitized solar cell for indoor applications: a mini-review," *Journal of Electronic Materials*, vol. 50, no. 6, pp. 3187–3206, 2021.

[34] B. Li, B. Hou, and G. A. J. Amaratunga, "Indoor photovoltaics, *the next big trend* in solution-processed solar cells," *InfoMat*, vol. 3, no. 5, pp. 445–459, 2021.

[35] E. Muchuweni, B. S. Martincigh, and V. O. Nyamori, "Recent advances in graphene-based materials for dye-sensitized solar cell fabrication," *RSC Advances*, vol. 10, no. 72, pp. 44453–44469, 2020.

[36] J. Highfield, "Advances and recent trends in heterogeneous photo(electro)-catalysis for solar fuels and chemicals," *Molecules*, vol. 20, no. 4, pp. 6739–6793, 2015.

[37] A. Pareek, A. Gopalakrishnan, and P. H. Borse, "Reduced graphene oxide decorated Tio2 for improving dye-sensitized solar cells," *Journal of Physics: Conference Series*, vol. 755, no. 1, article 012006, 2016.

[38] V. Rondán-Gómez, I. M. D. L. Santos, D. Seuret-Jiménez et al., "Recent advances in dye-sensitized solar cells," *Applied Physics A - Materials Science & Processing*, vol. 125, no. 12, pp. 1–24, 2019.

[39] S. Datta, A. Dey, N. R. Singha, and S. Roy, "Enhanced performance of dye-sensitized solar cell with thermally stable natural dye-assisted TiO_2/MnO_2 bilayer-assembled photoanode," *Materials for Renewable and Sustainable Energy*, vol. 9, no. 4, 2020.

[40] A. Andualem and S. Demiss, *Review on dye-sensitized solar cells (DSSCs)*, Edelweiss Applied Science and Technology, 2018.

[41] D. Ghernaout, A. Boudjemline, and N. Elboughdiri, "Electrochemical engineering in the core of the dye-sensitized solar cells (DSSCs)," *Open Access Library Journal*, vol. 7, no. 3, pp. 1–12, 2020.

[42] R. Rajendhiran, V. Deivasigamani, J. Palanisamy, S. Pitchaiya, N. Eswaramoorthy, and S. Masan, "*Plectranthus amboinicus* leaf extract synthesized spherical like-TiO_2 photoanode for dye-sensitized solar cell application," *SILICON*, vol. 13, no. 10, pp. 3329–3336, 2021.

[43] L. Wei, P. Wang, Y. Yang, R. Fan, Y. Yang, and Y. Qiu, "Construction of efficient photoanodes for dye sensitized solar cells: TiO_2 films with a gradient content of graphene," *Sustainable Energy and Fuels*, vol. 1, no. 5, pp. 1112–1122, 2017.

[44] F. W. Low and C. W. Lai, "Reduced graphene oxide decorated Tio2 for improving dye-sensitized solar cells (DSSCs)," *Current Nanoscience*, vol. 15, no. 6, pp. 631–636, 2019.

[45] N. Gao, T. Wan, Z. Xu, L. Ma, S. Ramakrishna, and Y. Liu, "Nitrogen doped TiO_2/graphene nanofibers as DSSCs photoanode," *Materials Chemistry and Physics*, vol. 255, article 123542, 2020.

[46] S. Thambidurai, P. Gowthaman, M. Venkatachalam, S. Suresh, and M. Kandasamy, "Morphology dependent photovoltaic performance of zinc oxide-cobalt oxide nanoparticle/nanorod composites synthesized by simple chemical co-precipitation method," *Journal of Alloys and Compounds*, vol. 852, article 156997, 2021.

[47] H. A. Maddah, V. Berry, and S. K. Behura, "Biomolecular photosensitizers for dye-sensitized solar cells: recent developments and critical insights," *Renewable and Sustainable Energy Reviews*, vol. 121, no. January, article 109678, 2020.

[48] P. Huang, S. Xu, M. Zhang, W. Zhong, Z. Xiao, and Y. Luo, "Lotus leaf derived natural dye as sensitizer and biochar as counter electrode for dye-sensitized solar cells," *Materials Science Forum*, vol. 993, pp. 884–892, 2020.

[49] G. F. C. Mejica, Y. Unpaprom, and R. Ramaraj, "Fabrication and performance evaluation of dye-sensitized solar cell integrated with natural dye from Strobilanthes cusia under different counter-electrode materials," *Applied Nanoscience*, 2021.

[50] R. Kumar, V. Sahajwalla, and P. Bhargava, "Fabrication of a counter electrode for dye-sensitized solar cells (DSSCs) using a carbon material produced with the organic ligand 2-methyl-8-hydroxyquinolinol (Mq)," *nanoscale advances*, vol. 1, no. 8, pp. 3192–3199, 2019.

[51] M. Younas, T. N. Baroud, M. A. Gondal, M. A. Dastageer, and E. P. Giannelis, "Highly efficient, cost-effective counter electrodes for dye-sensitized solar cells (DSSCs) augmented by highly mesoporous carbons," *Journal of Power Sources*, vol. 468, no. June, article 228359, 2020.

[52] C. Song, S. Wang, W. Dong et al., "Hydrothermal synthesis of iron pyrite (FeS_2) as efficient counter electrodes for dye-sensitized solar cells," *Solar Energy*, vol. 133, pp. 429–436, 2016.

[53] H. P. Kim, A. R. Yusoff, H. M. Kim, H. J. Lee, G. J. Seo, and J. Jang, "Inverted organic photovoltaic device with a new electron transport layer," *Nanoscale research letters*, vol. 9, no. 1, pp. 1–9, 2014.

[54] S. Sowmya, P. Prakash, N. Ruba, B. Janarthanan, A. Nagamani Prabu, and J. Chandrasekaran, "A study on

the fabrication and characterization of dye-sensitized solar cells with *Amaranthus red* and *Lawsonia inermis* as sensitizers with maximum absorption of visible light," *Journal of Materials Science: Materials in Electronics*, vol. 31, no. 8, pp. 6027–6035, 2020.

[55] D. D. Pratiwi, F. Nurosyid, A. Supriyanto, and R. Suryana, "Optical properties of natural dyes on the dye-sensitized solar cells (DSSC) performance," *Journal of Physics: Conference Series*, vol. 776, no. 1, article 012007, 2016.

[56] I. Gradzka-Kurzaj, M. Gierszewski, G. Burdzinski, and M. Zioek, "Interplay between ruthenium sensitizer and ruthenium catalyst in photoelectrochemical cells with different water-based electrolytes," *Journal of Physical Chemistry C*, vol. 124, no. 39, pp. 21268–21282, 2020.

[57] A. Mahmood, "Recent research progress on quasi-solid-state electrolytes for dye-sensitized solar cells," *Journal of Energy Chemistry*, vol. 24, no. 6, pp. 686–692, 2015.

[58] U. Mehmood, S. U. Rahman, K. Harrabi, I. A. Hussein, and B. V. S. Reddy, "Recent advances in dye sensitized solar cells," *Advances in Materials Science and Engineering*, vol. 2014, Article ID 974782, 12 pages, 2014.

[59] N. Wang, J. Hu, L. Gao, and T. Ma, "Current progress in solid-state electrolytes for dye-sensitized solar cells: a mini-review," *Journal of Electronic Materials*, vol. 49, no. 12, pp. 7085–7097, 2020.

[60] V. Selvanathan, R. Yahya, M. Shahiduzzaman et al., "Ionic liquid infused starch-cellulose derivative based quasi-solid dye-sensitized solar cell: exploiting the rheological properties of natural polymers," *Cellulose*, vol. 28, no. 9, pp. 5545–5557, 2021.

[61] F. I. Saaid, T. Y. Tseng, and T. Winie, "PVdF-HFP quasi-solid-state electrolyte for application in dye-sensitized solar cells," *International Journal of Technology*, vol. 9, no. 6, pp. 1187–1195, 2018.

[62] J. M. Lim, J. Park, J. T. Park, and S. Bae, "Preparation of quasi-solid-state electrolytes using a coal fly ash derived zeolite-X and -A for dye-sensitized solar cells," *Journal of Industrial and Engineering Chemistry*, vol. 71, pp. 378–386, 2019.

[63] J. Yin, "The application of natural dyes in dye-sensitized solar cells," in *Proceedings of the 2016 6th International Conference on Machinery, Materials, Environment, Biotechnology and Computer*, pp. 1297–1300, Atlantis Press, Paris, France, 2016.

[64] N. Mariotti, M. Bonomo, L. Fagiolari et al., "Recent advances in eco-friendly and cost-effective materials towards sustainable dye-sensitized solar cells," *Green Chemistry*, vol. 22, no. 21, pp. 7168–7218, 2020.

[65] M. R. Nalzala Thomas, V. J. Kanniyambatti Lourdusamy, A. A. Dhandayuthapani, and V. Jayakumar, "Non-metallic organic dyes as photosensitizers for dye-sensitized solar cells: a review," *Environmental Science and Pollution Research*, vol. 28, no. 23, pp. 28911–28925, 2021.

[66] P. Trihutomo, S. Soeparman, D. Widhiyanuriyawan, and L. Yuliati, "Performance improvement of dye-sensitized solar cell- (DSSC-) based natural dyes by clathrin protein," *International Journal of Photoenergy*, vol. 2019, Article ID 4384728, 9 pages, 2019.

[67] H. Hug, M. Bader, P. Mair, and T. Glatzel, "Biophotovoltaics: natural pigments in dye-sensitized solar cells," *Applied Energy*, vol. 115, pp. 216–225, 2014.

[68] L. Li, K. Zhao, and Y. Zhang, "Research progress of solar cells with natural dyes constructed as sensitizer," in *Proceedings of the 2016 International Conference on Civil, Structure and Environmental Engineering*, pp. 106–110, Atlantis Press, Paris, France, 2016.

[69] S. Sreeja and B. Pesala, "Performance enhancement of beta-nin solar cells co-sensitized with indigo and lawsone: a comparative study," *ACS Omega*, vol. 4, no. 19, pp. 18023–18034, 2019.

[70] S. Ananthakumar, D. Balaji, J. Ram Kumar, and S. Moorthy Babu, *Role of Co-Sensitization in Dye-Sensitized and Quantum Dot-Sensitized Solar Cells*, vol. 1, no. 2, 2019Springer International Publishing, 2019.

[71] I. McConnell, G. Li, and G. W. Brudvig, "Energy conversion in natural and artificial photosynthesis," *Chemistry & Biology*, vol. 17, no. 5, pp. 434–447, 2010.

[72] J. J. Marizcurrena, S. Castro-Sowinski, and M. F. Cerdá, "Improving the performance of dye-sensitized solar cells using nanoparticles and a dye produced by an Antarctic bacterium," *Environmental Sustainability*, vol. 4, no. 4, pp. 711–721, 2021.

[73] N. E. Safie, N. A. Ludin, N. H. Hamid et al., "Electron transport studies of dye-sensitized solar cells based on natural sensitizer extracted from rengas (Gluta spp.) and mengkulang (Heritiera elata) wood," *BioResources*, vol. 12, no. 4, pp. 9227–9243, 2017.

[74] P. Khammee, Y. Unpaprom, T. Thurakitseree, N. Dussadee, S. Kojinok, and R. Ramaraj, "Natural dyes extracted from Inthanin bok leaves as light-harvesting units for dye-sensitized solar cells," *Applied Nanoscience*, pp. 1–13, 2021.

[75] H. Jaafar, M. F. Ain, and Z. A. Ahmad, "Performance of *E. conferta* and *G. atroviridis* fruit extracts as sensitizers in dye-sensitized solar cells (DSSCs)," *Ionics (Kiel)*, vol. 24, no. 3, pp. 891–899, 2018.

[76] M. Khalili, M. Abedi, and H. S. Amoli, "Influence of saffron carotenoids and mulberry anthocyanins as natural sensitizers on performance of dye-sensitized solar cells," *Ionics (Kiel)*, vol. 23, no. 3, pp. 779–787, 2017.

[77] D. N. F. P. Damit, K. Galappaththi, A. Lim, M. I. Petra, and P. Ekanayake, "Formulation of water to ethanol ratio as extraction solvents of *Ixora coccinea* and *Bougainvillea glabra* and their effect on dye aggregation in relation to DSSC performance," *Ionics (Kiel)*, vol. 23, no. 2, pp. 485–495, 2017.

[78] N. H. Hamid, S. Sepeai, M. A. Teridi, M. A. Ibrahim, K. Sopian, and H. Arakawa, "Energy levels of natural sensitizers extracted from rengas (*Gluta* spp.) and mengkulang (*Heritiera elata*) wood for dye-sensitized solar cells," *Materials for Renewable and Sustainable Energy*, vol. 6, no. 2, pp. 1–9, 2017.

[79] N. Prabavathy, S. Shalini, R. Balasundaraprabhu, D. Velauthapillai, S. Prasanna, and N. Muthukumarasamy, "Enhancement in the photostability of natural dyes for dye-sensitized solar cell (DSSC) applications: a review," *International Journal of Energy Research*, vol. 41, no. 10, pp. 1372–1396, 2017.

[80] N. Prabavathy, S. Shalini, R. Balasundaraprabhu et al., "Effect of solvents in the extraction and stability of anthocyanin from the petals of *Caesalpinia pulcherrima* for natural dye sensitized solar cell applications," *Journal of Materials Science: Materials in Electronics*, vol. 28, no. 13, pp. 9882–9892, 2017.

[81] J. H. Kim and S. H. Han, "Energy generation performance of window-type dye-sensitized solar cells by color and transmittance," *Sustainability*, vol. 12, no. 21, pp. 1–13, 2020.

[82] R. Senthamarai, V. Madurai Ramakrishnan, B. Palanisamy, and S. Kulandhaivel, "Synthesis of TiO_2 nanostructures by green approach as photoanodes for dye-sensitized solar cells," *International Journal of Energy Research*, vol. 45, no. 2, pp. 3089–3096, 2021.

[83] N. Y. Amogne, D. W. Ayele, and Y. A. Tsigie, "Recent advances in anthocyanin dyes extracted from plants for dye sensitized solar cell," *Materials for Renewable and Sustainable Energy*, vol. 9, no. 4, pp. 1–16, 2020.

[84] N. Aziz, N. A. Mat Nor, and A. K. Arof, "Optimization of anthocyanin extraction parameters from *M. malabathricum* via response surface methodology to produce natural sensitizer for dye sensitized solar cells," *Optical and Quantum Electronics*, vol. 52, no. 1, pp. 1–13, 2020.

[85] M. A. M. Al-Alwani, N. A. Ludin, A. B. Mohamad, A. A. H. Kadhum, M. M. Baabbad, and K. Sopian, "Optimization of dye extraction from *Cordyline fruticosa* via response surface methodology to produce a natural sensitizer for dye-sensitized solar cells," *Results in physics*, vol. 6, no. August, pp. 520–529, 2016.

[86] D. Sinha, D. De, and A. Ayaz, "Photo sensitizing and electrochemical performance analysis of mixed natural dye and nanostructured ZnO based DSSC," *Sadhana - Academy Proceedings in Engineering Sciences*, vol. 45, no. 1, p. 175, 2020.

[87] G. M. Lohar, D. V. Rupnawar, R. V. Shejawal, and A. V. Fulari, "Preparation of natural dyes from salvia and spathodea for TiO_2-based dye-sensitized solar cells (DSSCs) and their electrochemical impedance spectroscopic study under light and dark conditions," *Bulletin of Materials Science*, vol. 43, no. 1, pp. 1–8, 2020.

[88] T. Raguram and K. S. Rajni, "Characterization of TiO_2 photoanodes and natural dyes (Allamanda blanchetti and Allamanda cathartica) extract as sensitizers for dye-sensitized solar cell applications," *Journal of Sol-Gel Science and Technology*, vol. 93, no. 1, pp. 202–213, 2020.

[89] P. Khammee, Y. Unpaprom, K. Whangchai, and R. Ramaraj, "Comparative studies of the longan leaf pigment extraction as a photosensitizer for dye-sensitized solar cells' purpose," *Biomass Conversion and Biorefinery*, vol. 12, no. 5, pp. 1619–1626, 2022.

[90] S. S. Sahoo, S. Salunke-Gawali, V. S. Kadam, and H. M. Pathan, "Canna lily red and yellow flower extracts: a new power source to produce photovoltage through dye-sensitized solar cells," *Energy & Fuels*, vol. 34, no. 8, pp. 9674–9682, 2020.

[91] T. Shanmugapriya and J. Balavijayalakshmi, "Efficiency studies of Galinsoga parviflora pigments as a sensitizer in Pt free graphene oxide/nickel oxide counter electrode: dye sensitized solar cell applications," *Journal of Cluster Science*, vol. 32, no. 5, pp. 1277–1288, 2021.

[92] Q. Liu, N. Gao, D. Liu, J. Liu, and Y. Li, "Structure and photo-electrical properties of natural photoactive dyes for solar cells," *Applied Sciences*, vol. 8, no. 9, p. 1697, 2018.

[93] D. Ganta, J. Jara, and R. Villanueva, "Dye-sensitized solar cells using aloe vera and cladode of cactus extracts as natural sensitizers," *Chemical Physics Letters*, vol. 679, pp. 97–101, 2017.

[94] A. K. Rajan and L. Cindrella, "A study on the performance of dye sensitized solar cells using extract from *Wrightia tinctoria* R.Br. as photosensitizers," *Journal of Electronic Materials*, vol. 48, no. 12, pp. 7647–7653, 2019.

[95] R. Hemmatzadeh and A. Mohammadi, "Improving optical absorptivity of natural dyes for fabrication of efficient dye-sensitized solar cells," *Journal of theoretical and applied physics*, vol. 7, no. 1, p. 57, 2013.

[96] M. A. Green, Y. Hishikawa, E. D. Dunlop et al., "Solar cell efficiency tables (version 53)," *Progress in Photovoltaics: Research and Applications*, vol. 27, no. 1, pp. 3–12, 2019.

[97] A. S. Najm, N. A. Ludin, M. F. Abdullah, M. A. Almessiere, N. M. Ahmed, and M. A. M. Al-Alwani, "*Areca catechu* extracted natural new sensitizer for dye-sensitized solar cell: performance evaluation," *Journal of Materials Science: Materials in Electronics*, vol. 31, no. 4, pp. 3564–3575, 2020.

[98] W. Ghann, H. Kang, T. Sheikh et al., "Fabrication, optimization and characterization of natural dye sensitized solar cell," *Scientific reports*, vol. 7, no. 1, article 41470, 2017.

[99] I. K. Mohammed and I. K. Uthman, "The effect on extracting solvents using natural dye extracts from Hyphaene thebaica for dye-sensitized solar cells," *Journal of Materials Science and Engineering*, vol. 5, no. 1, pp. 4–6, 2015.

[100] D. M. Sampaio, R. S. Babu, H. R. M. Costa, and A. L. F. de Barros, "Investigation of nanostructured TiO_2 thin film coatings for DSSCs application using natural dye extracted from jabuticaba fruit as photosensitizers," *Ionics (Kiel)*, vol. 25, no. 6, pp. 2893–2902, 2019.

[101] A. Arulraj, S. Govindan, S. Vadivel, and B. Subramanian, "Photovoltaic performance of TiO_2 using natural sensitizer extracted from *Phyllanthus reticulatus*," *Journal of Materials Science: Materials in Electronics*, vol. 28, no. 24, pp. 18455–18462, 2017.

[102] S. K. Das, S. Ganguli, H. Kabir, J. I. Khandaker, and F. Ahmed, "Performance of natural dyes in dye-sensitized solar cell as photosensitizer," *Transactions on Electrical and Electronic Materials*, vol. 21, no. 1, pp. 105–116, 2020.

[103] P. Enciso and M. F. Cerdá, "Solar cells based on the use of photosensitizers obtained from Antarctic red algae," *Cold Regions Science and Technology*, vol. 126, pp. 51–54, 2016.

[104] J. Ramirez-Perez, C. Maria, and C. P. Santacruz, "Impact of solvents on the extraction and purification of vegetable dyes onto the efficiency for dye-sensitized solar cells," *Renewables: Wind, Water, and Solar*, vol. 6, no. 1, 2019.

[105] L. A. DeSilva, P. K. Pitigala, A. Gaquere-Parker et al., "Broad absorption natural dye (Mondo-Grass berry) for dye sensitized solar cell," *Journal of Materials Science: Materials in Electronics*, vol. 28, no. 11, pp. 7724–7729, 2017.

[106] A. Listorti, B. O'Regan, and J. R. Durrant, "Electron transfer dynamics in dye-sensitized solar cells," *Chemistry of Materials*, vol. 23, no. 15, pp. 3381–3399, 2011.

[107] U. Banin, N. Waiskopf, L. Hammarström et al., "Nanotechnology for catalysis and solar energy conversion," *Nanotechnology*, vol. 32, no. 4, article 042003, 2020.

[108] S. Akin, S. Açikgöz, M. Gülen, C. Akyürek, and S. Sönmezoğlu, "Investigation of the photoinduced electron injection processes for natural dye-sensitized solar cells: the impact of anchoring groups," *RSC Advances*, vol. 6, no. 88, pp. 85125–85134, 2016.

[109] C. Cavallo, F. Di Pascasio, A. Latini, M. Bonomo, and D. Dini, "Nanostructured semiconductor materials for dye-sensitized solar cells," *Journal of Nanomaterials*, vol. 2017, Article ID 5323164, 31 pages, 2017.

[110] C. Y. Chien and B. D. Hsu, "Optimization of the dye-sensitized solar cell with anthocyanin as photosensitizer," *Solar energy*, vol. 98, no. PC, pp. 203–211, 2013.

[111] N. E. H. Diyanahesa, A. Supriyanto, and A. H. Ramelan, "Improvement of efficiency of dye-sensitized solar cells (DSSC) transparent by optimizing of anthocyanin dyes hybrid dyenamo yellow (DN-F01)," *AIP Conference Proceedings*, vol. 2217, no. 1, article 030182, 2020.

[112] P. Selvaraj, H. Baig, T. K. Mallick et al., "Enhancing the efficiency of transparent dye-sensitized solar cells using concentrated light," *Solar Energy Materials and Solar Cells*, vol. 175, no. July 2017, pp. 29–34, 2018.

[113] M. J. García-Salinas and M. J. Ariza, "Optimizing a simple natural dye production method for dye-sensitized solar cells: examples for betalain (bougainvillea and beetroot extracts) and anthocyanin dyes," *Applied Sciences*, vol. 9, no. 12, p. 2515, 2019.

[114] E. T. Bekele, E. A. Zereffa, N. S. Gultom, D. H. Kuo, B. A. Gonfa, and F. K. Sabir, "Biotemplated synthesis of titanium oxide nanoparticles in the presence of root extract of *Kniphofia schemperi* and its application for dye sensitized solar cells," *International Journal of Photoenergy*, vol. 2021, Article ID 6648325, 12 pages, 2021.

[115] W. Xie, E. Pakdel, Y. Liang et al., "Natural eumelanin and its derivatives as multifunctional materials for bioinspired applications: a review," *Biomacromolecules*, vol. 20, no. 12, pp. 4312–4331, 2019.

[116] N. A. Norhisamudin, N. Sabani, M. M. Shamimin et al., "The effect of different solvents in natural dyes from roselle (Hibiscus sabdariffa) and green tea leaves (Camellia sinensis) for dye-sensitized solar cell," *Journal of Physics: Conference Series*, vol. 1755, no. 1, article 012024, 2021.

[117] I. O. Onuigbo, G. N. Abdulrahman, C. Onwujiuba, O. Iwu, M. F. Yahaya, and W. J. Jahng, "Magnesium-doped green solar cells using natural chromophores," *International Nano Letters*, vol. 11, no. 3, pp. 205–214, 2021.

[118] S. Kar, J. K. Roy, and J. Leszczynski, "In silico designing of power conversion efficient organic lead dyes for solar cells using todays innovative approaches to assure renewable energy for future," *NPJ Computational Materials*, vol. 3, no. 1, p. 22, 2017.

[119] V. Mohankumar, P. Pounraj, M. Senthil Pandian, and P. Ramasamy, "Theoretical investigation on flavones and isoflavones-added triphenylamine-based sensitizers for DSSC application," *Brazilian Journal of Physics*, vol. 49, no. 1, pp. 103–112, 2019.

[120] M. F. Maahury and M. A. Martoprawiro, "Computational study of anthocyanin as active material in dye-sensitized solar cell," *Journal of Physics: Conference Series*, vol. 1463, no. 1, article 012014, 2020.

[121] W. Zhang, L. Wang, L. Mao et al., "Computational protocol for precise prediction of dye-sensitized solar cell performance," *Journal of Physical Chemistry C*, vol. 124, no. 7, pp. 3980–3987, 2020.

[122] A. Ndiaye, A. Dioum, C. I. Oprea et al., "A combined experimental and computational study of chrysanthemin as a pigment for dye-sensitized solar cells," *Molecules*, vol. 26, no. 1, p. 225, 2021.

[123] K. Cvetanovic Zobenica, U. Lacnjevac, M. Etinski, D. Vasiljevic-Radovic, and D. Stanisavljev, "Influence of the electron donor properties of hypericin on its sensitizing ability in DSSCs," *Photochemical & Photobiological Sciences*, vol. 18, no. 8, pp. 2023–2030, 2019.

[124] S. Sreeja and B. Pesala, "Co-sensitization aided efficiency enhancement in betanin–chlorophyll solar cell," *Materials for Renewable and Sustainable Energy*, vol. 7, no. 4, p. 25, 2018.

[125] M. Xie, J. Wang, H. Q. Xia et al., "Theoretical studies on the spectroscopic properties of porphyrin derivatives for dye-sensitized solar cell application," *RSC Advances*, vol. 5, no. 42, pp. 33653–33665, 2015.

[126] D. R. Shinde, P. S. Tambade, K. M. Gadave, K. S. Pawar, M. Naushad, and H. M. Pathan, "Dye-sensitised solar cells with a naturally occurring pigment lycopene as a photosensitiser for zirconium dioxide: an experimental and theoretical study," *Journal of Materials Science: Materials in Electronics*, vol. 28, no. 15, pp. 11311–11316, 2017.

[127] M. Hosseinnezhad, K. Gharanjig, M. K. Yazdi et al., "Dye-sensitized solar cells based on natural photosensitizers: a green view from Iran," *Journal of Alloys and Compounds*, vol. 828, no. 2, article 154329, 2020.

[128] S. Tontapha, W. Sang-aroon, S. Kanokmedhakul, T. Promgool, and V. Amornkitbamrung, "Effects of dye-adsorption solvents, acidification and dye combination on efficiency of DSSCs sensitized by α-mangostin and anthocyanin from mangosteen pericarp," *Journal of Materials Science: Materials in Electronics*, vol. 28, no. 10, pp. 7454–7467, 2017.

[129] W. Maiaugree, S. Lowpa, M. Towannang et al., "A dye sensitized solar cell using natural counter electrode and natural dye derived from mangosteen peel waste," *Scientific reports*, vol. 5, no. 1, article 15230, 2015.

[130] C. Mebrahtu, A. M. Taddesse, G. Goro, and T. Yohannes, "Natural pigment sensitized solar cells based on ZnO-TiO$_2$-Fe$_2$O$_3$ nanocomposite in quasi-solid state electrolyte system," *Bulletin of the Chemical Society of Ethiopia*, vol. 31, no. 2, pp. 263–279, 2017.

[131] K. C. Cho, H. Chang, C. H. Chen, M. J. Kao, and X. R. Lai, "A study of mixed vegetable dyes with different extraction concentrations for use as a sensitizer for dye-sensitized solar cells," *International Journal of Photoenergy*, vol. 2014, Article ID 492747, 5 pages, 2014.

[132] H. Lv, X. Yuan, and C. Cui, "Enhancing the photovoltaic performance of dye-sensitized solar cells by modifying TiO$_2$ photoanodes with layered structure g-C3N4," *AIP Conference Proceedings*, vol. 1820, no. 1, 2017.

[133] M. Z. Najibah and W. Tan, "Dye extracted from Costus woodsonii leave as a natural sensitizer for dye-sensitized solar cell," *Science Letters (ScL)*, vol. 15, no. 1, pp. 58–68, 2021.

[134] M. A. M. Al-Alwani, A. B. Mohamad, A. A. H. Kadhum et al., "Natural dye extracted from Pandannus amaryllifolius leaves as sensitizer in fabrication of dye-sensitized solar cells," *International Journal of Electrochemical Science*, vol. 12, no. 1, pp. 747–761, 2017.

[135] S. Bera, D. Sengupta, S. Roy, and K. Mukherjee, "Research into dye-sensitized solar cells: a review highlighting progress in India," *Journal of Physics: Energy*, vol. 3, no. 3, article 032013, 2021.

[136] O. I. Francis and A. Ikenna, "Review of dye-sensitized solar cell (DSSCs) development," *Natural Science*, vol. 13, no. 12, pp. 496–509, 2021.

[137] Y. Wen, L. Fu, G. Li, J. Ma, and H. Ma, "Accelerated discovery of potential organic dyes for dye-sensitized solar cells by

interpretable machine learning models and virtual screening," *Solar RRL*, vol. 4, no. 6, article 2000110, 2020.

[138] A. Aslam, U. Mehmood, M. H. Arshad et al., "Dye-sensitized solar cells (DSSCs) as a potential photovoltaic technology for the self-powered internet of things (IoTs) applications," *Solar Energy*, vol. 207, pp. 874–892, 2020.

[139] N. R. Bader, "Sample preparation for flame atomic absorption spectroscopy: an overview," *Rasayan Journal of Chemistry*, vol. 4, no. 1, pp. 49–55, 2011.